

Supporting Information
Ruthenium polyhydrides supported by rigid PCP pincer ligands: dynamic behaviour and reactions with
CO₂

Laurie J. Donnelly, Jian-Bin Lin, Benjamin S. Gelfand, Chia Yun Chang and Warren E. Piers

Table of Contents

Figures Referenced in Manuscript.....	3
Figure S1	3
Figure S2	4
Figure S3	5
Figure S4	6
Figure S5	7
Figure S6	7
Figure S7	8
Table S1	9
Experimental Details.....	10
General Considerations	10
Synthesis of L_HRuCl₂	10
Synthesis of L_{NMe₂}RuCl₂	10
Synthesis of L_HRu(H)Cl	11
Synthesis of L_{NMe₂}Ru(H)Cl :	11
Synthesis of L_{HH}Ru(H)₃/L_{HH}RuH	12
Synthesis of L_{NMe₂}Ru(H)₃/L_{HNMe₂}RuH :.....	12
Synthesis of L_{DNMe₂}Ru(D)₃	13
Characterization of [L_{HNMe₂}Ru(H)](μ-N₂)	13
Synthesis of L_HRu(H)-κ²-O₂CH	13
Synthesis of L_HRu(H)-κ²-O₂¹³CH :	14
Synthesis of L_{NMe₂}Ru(H)-κ²-O₂CH :.....	14
Synthesis of L_{NMe₂}Ru(H)-κ²-O₂¹³CH :.....	15
NMR Spectra.....	15
³¹ P{ ¹ H}, ¹ H and ¹³ C{ ¹ H} NMR for Characterization of Reported L_H Supported Compounds	15
³¹ P{ ¹ H}, ¹ H and ¹³ C{ ¹ H} NMR for Characterization of Reported L_{NMe₂} Supported Compounds	29
Variable Temperature NMR Spectra of L_{HH}Ru(H)₃	45

NMR Spectra of Isotopically Labelled Compounds.....	47
Determination of T_1 for $L_{HR}Ru(H)_3$.....	50
Crystal Structure Determination Data	50
General X-ray Diffraction Collection and Refinement Information	50
Additional XRD Determined Structures	52
Collection and Refinement Parameters for Included X-ray Diffraction Structures.....	53
References	55

Figures Referenced in Manuscript.

Figure S1

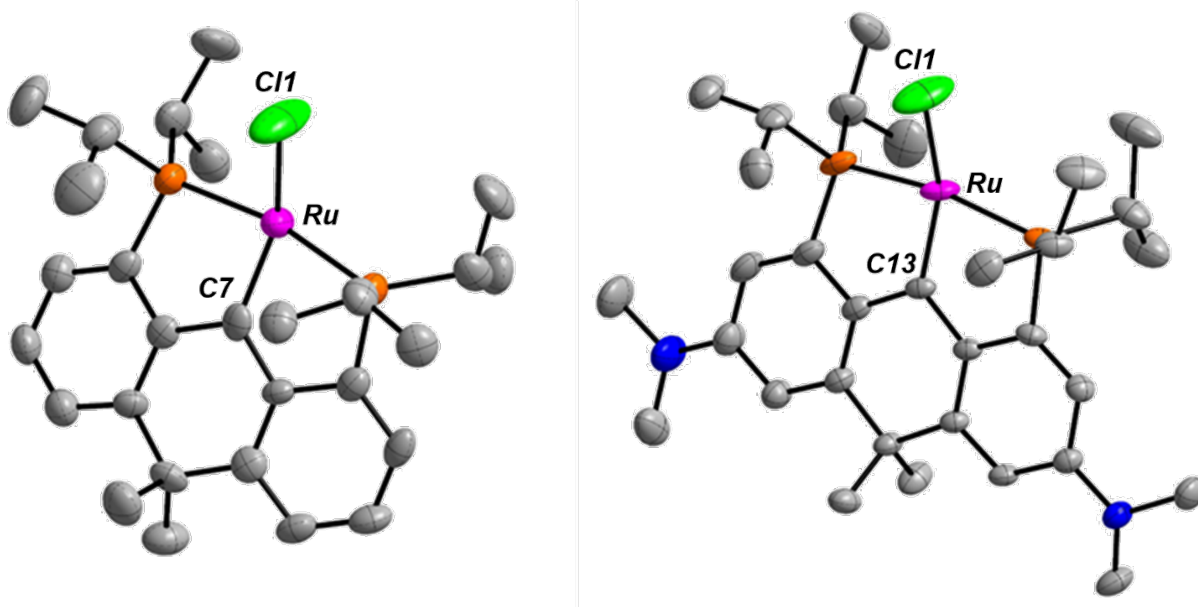


Figure S1: XRD determined structures of $L_HRu(H)Cl$ (left) and $L_{NMe_2}Ru(H)Cl$ (right), with thermal ellipsoids drawn at 50% probability level. Ligand H atoms omitted for clarity. Hydrides were not located in the difference map for either structure. Selected bond lengths [\AA] and bond angles [$^\circ$] for $L_HRu(H)Cl$: Ru1-C7: 1.93(1), Ru1-Cl1: 2.371(4); C7-Ru1-Cl1: 145.1(4). Selected bond lengths [\AA] and bond angles [$^\circ$] for $L_{NMe_2}Ru(H)Cl$: Ru1-C13: 1.9176(24), Ru1-Cl1: 2.4266(10), C13-Ru1-Cl1: 148.231(70).

Figure S2

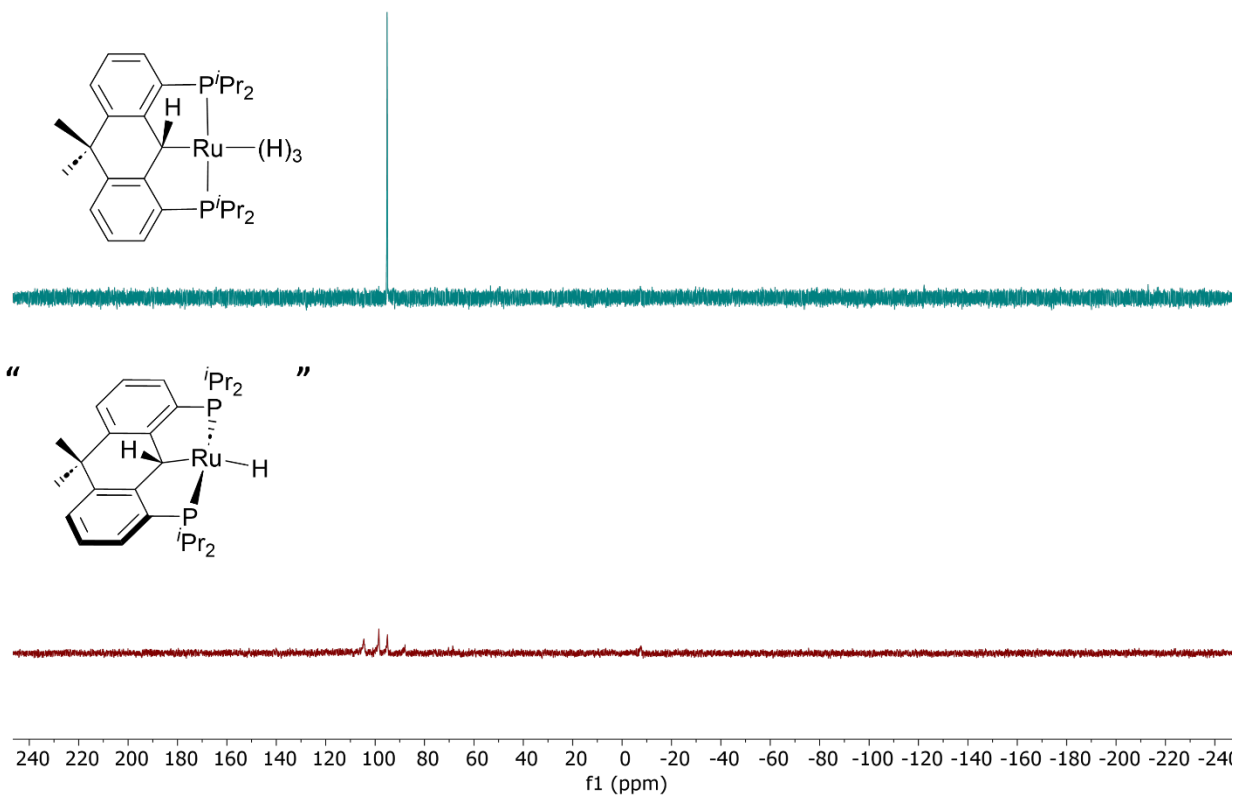


Figure S2: $^{31}\text{P}\{^1\text{H}\}$ NMR spectra of $\text{L}_{\text{HH}}\text{Ru}(\text{H})_3$ (top, under H_2) and $\text{L}_{\text{HH}}\text{RuH}$ (bottom, under argon) in C_6D_6 . Note: adding 1 atm of H_2 returns the top spectrum.

Figure S3

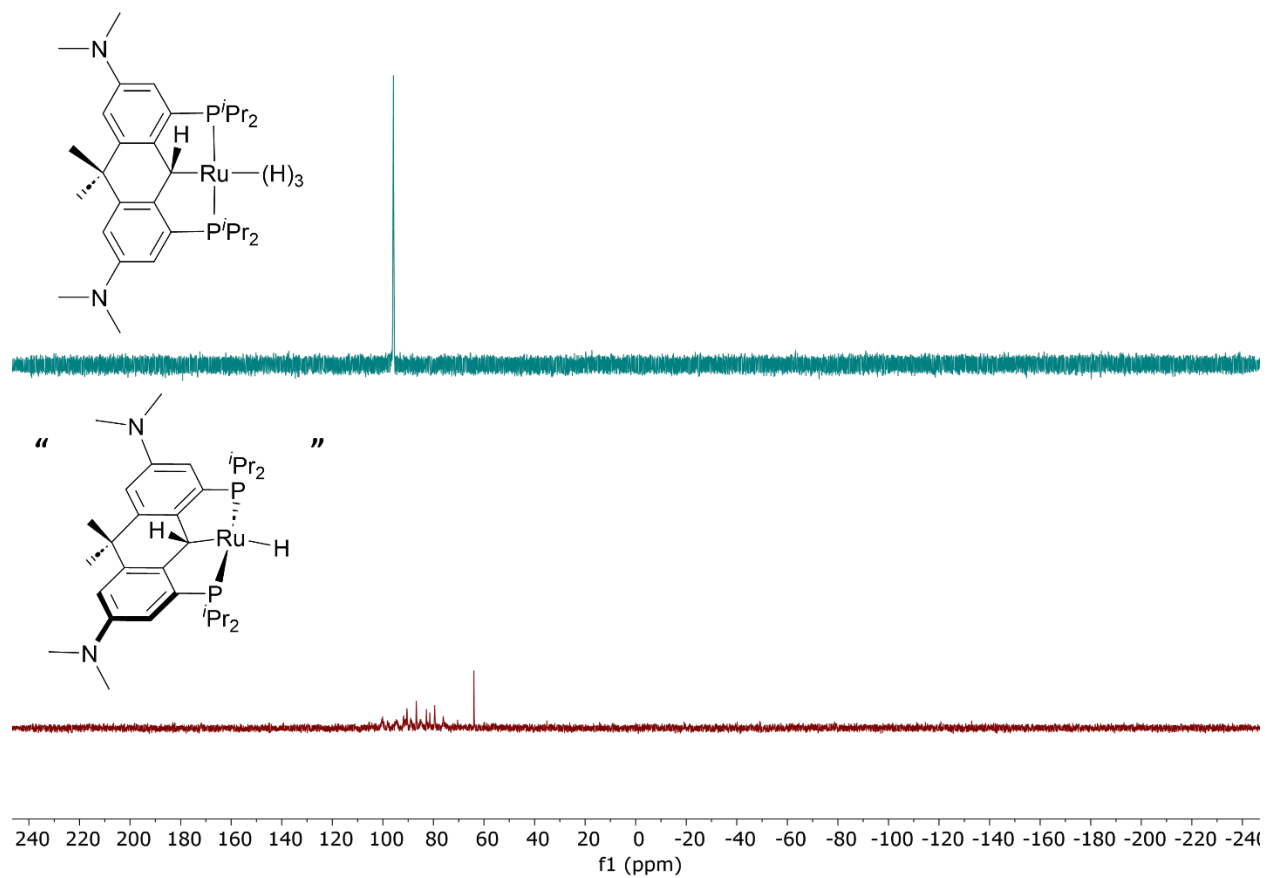


Figure S3: $^{31}\text{P}\{^1\text{H}\}$ NMR spectra of $\text{L}_{\text{HNMe}_2}\text{Ru}(\text{H})_3$ (top, under H_2) and $\text{L}_{\text{HNMe}_2}\text{RuH}$ (bottom, under argon) in C_6D_6 . Note: adding 1 atm of H_2 returns the top spectra.

Figure S4

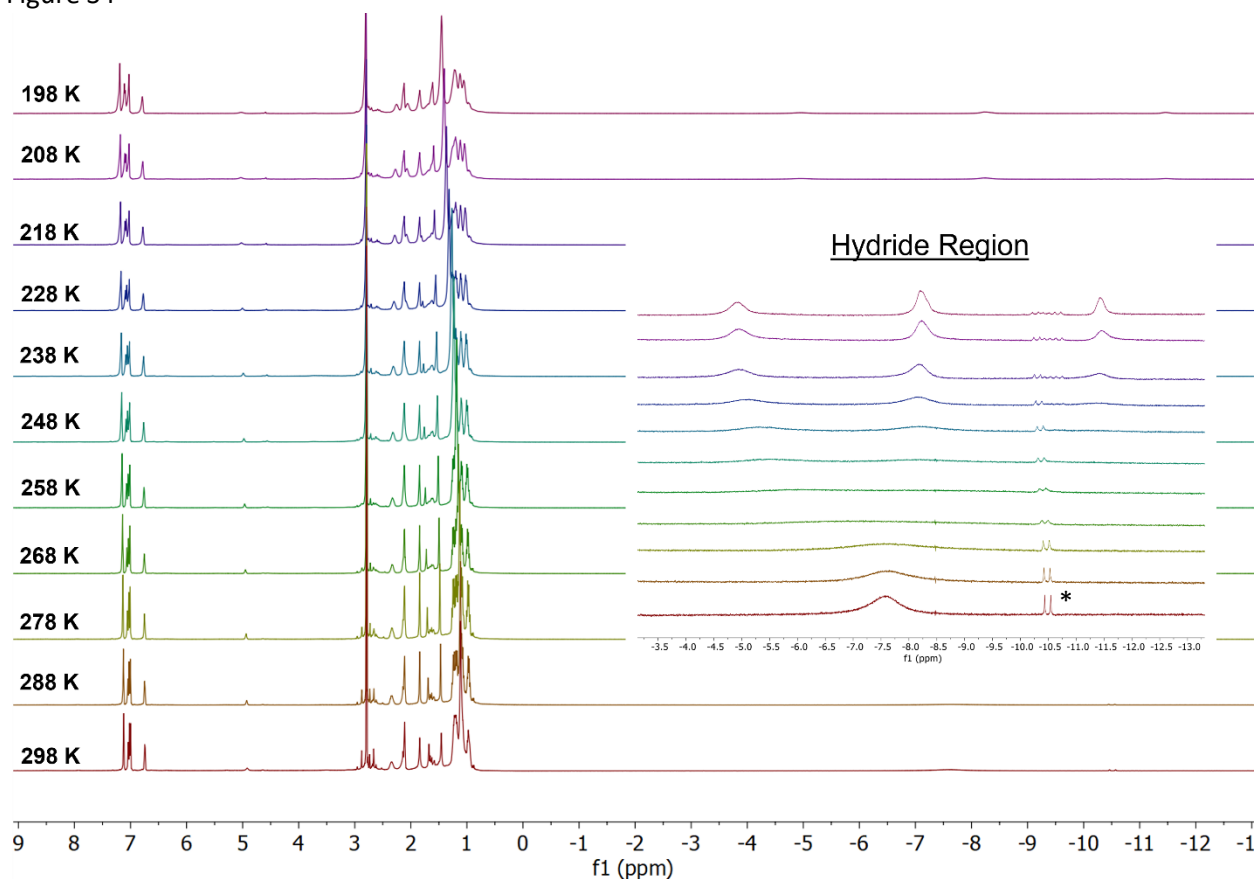


Figure S4: Variable temperature ^1H NMR spectrum of $\text{L}_{\text{HNMe}_2}\text{Ru}(\text{H})_3$ in toluene-d_8 under 1 atm H_2 . Hydride product at -10.5 ppm (*) undergoes a dynamic process but does not exchange with the main product as shown in the ^1H EXSY NMR spectrum (Figure S5). Variable temperature NMR for $\text{L}_{\text{HH}}\text{Ru}(\text{H})_3$ is shown below (Figure S39).

Figure S5

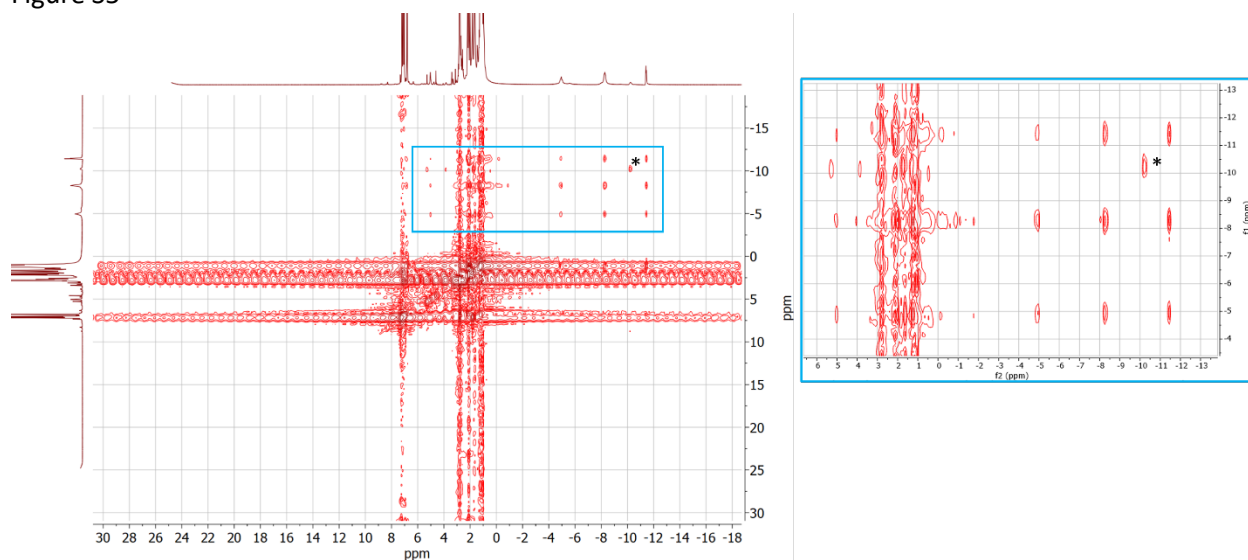


Figure S5: ^1H - ^1H EXSY NMR of $\text{L}_{\text{HNMe}_2}\text{Ru}(\text{H})_3$ at 200 K in toluene- d_8 , showing the minor product hydride resonance (*) that does not exchange with the $\text{L}_{\text{HNMe}_2}\text{Ru}(\text{H})_3$ resonances.

Figure S6

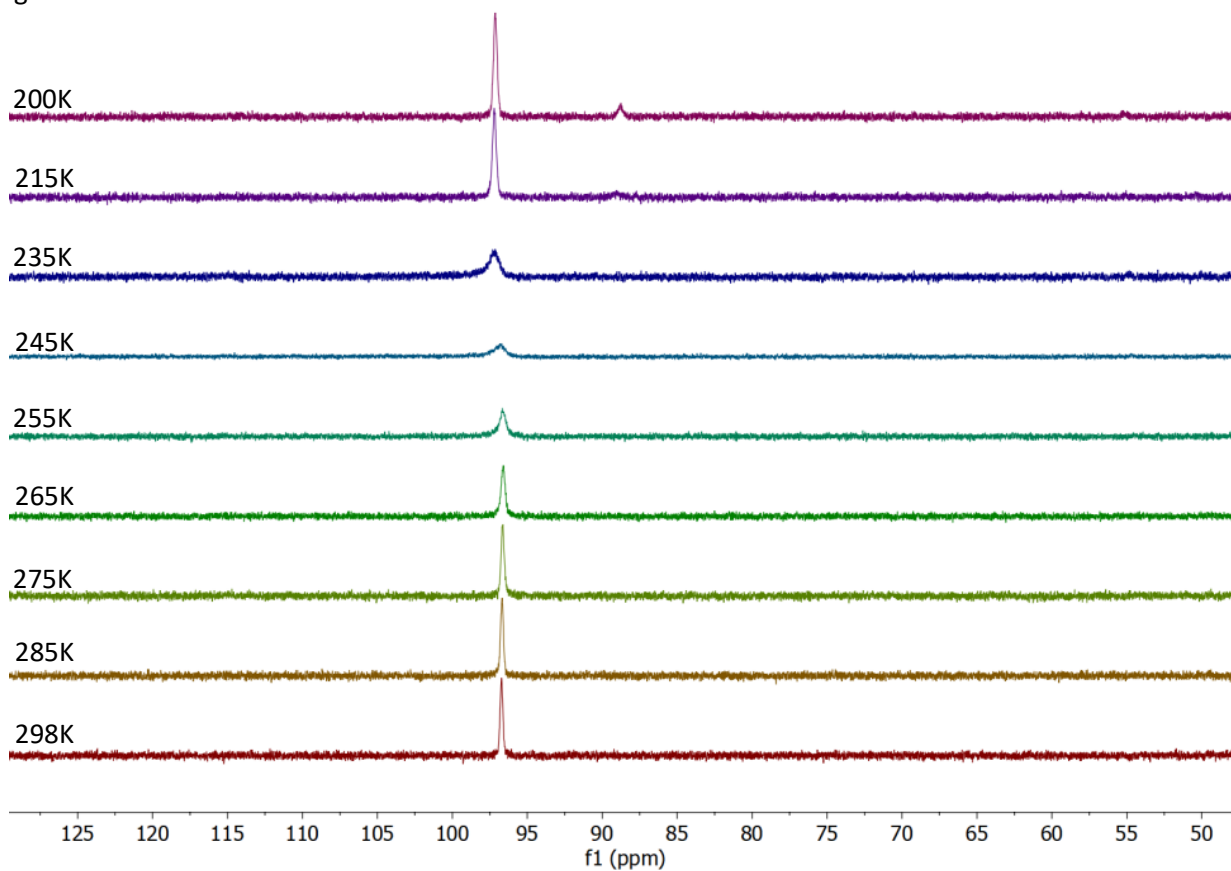


Figure S6: Variable temperature $^{31}\text{P}\{^1\text{H}\}$ NMR spectrum of $\text{L}_{\text{HNMe}_2}\text{Ru}(\text{H})_3$ in toluene- d_8 . Variable temperature NMR for $\text{L}_{\text{HH}}\text{Ru}(\text{H})_3$ is shown below (Figure S38).

Figure S7

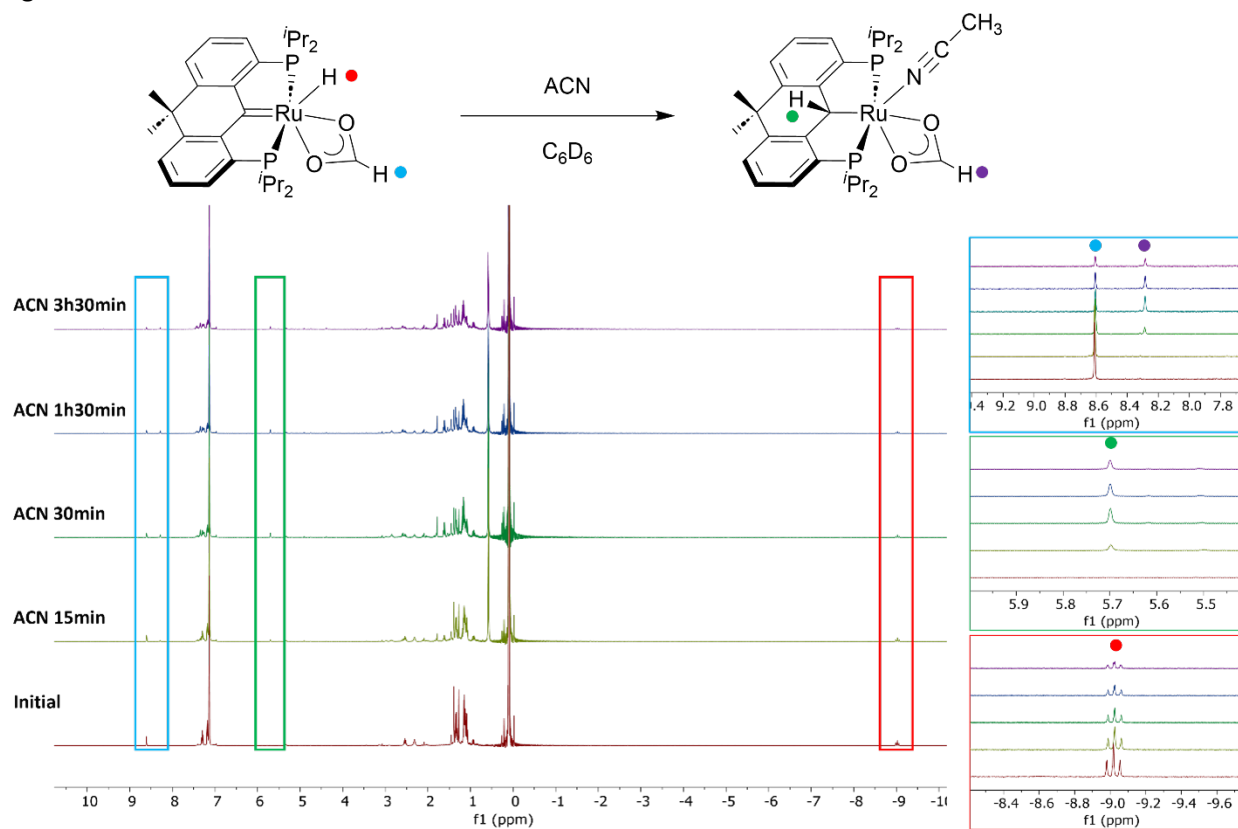
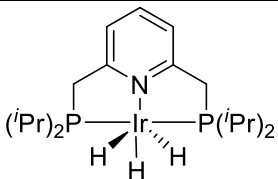
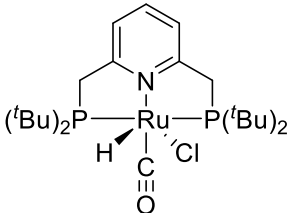
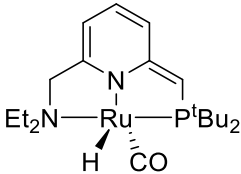
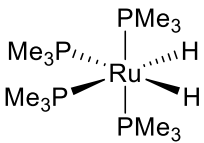
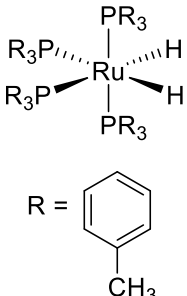


Figure S7: 1H NMR spectrum of $L_HRu(H)-\kappa^2-O_2CH$ in C_6D_6 with added acetonitrile. Highlighted boxes show new formate resonance (top), growing benzylic resonance (middle) and disappearing hydride resonance (bottom).

Table S1

Table S1: Select Examples of CO₂ hydrogenation catalysts. [a] TON/TOF determined in early phase of reaction.

Catalyst Precursor	Solvent	Base Additive	[Ratio H ₂ :CO ₂ /P _{tot} (bar)]	Temperature (°C)	time (h)	TON	TOF (h ⁻¹)	Ref
	THF	KOH	1:1 / 60	120	48	3.5*10 ⁶	7.3*10 ⁵	1
	DMF	DBU	3:1/ 40	120	0.4 ^[a]	2.0*10 ⁵	1.1*10 ⁶	2
	diglyme	K ₂ CO ₃	4:1 / 10	200	48	2.3*10 ⁴	2200	3
	scCO ₂	NEt ₃	17:24 / 205	50	1	7200	1400	4
	2:1 dioxane:water	KOH	1:1/ 60	40	3	240 ^[a]	46	5

Experimental Details

General Considerations

Storage and manipulation of all compounds was performed under an argon atmosphere either in a VAC glove box or using a double manifold high vacuum line using standard techniques. Passage of argon through an OxisorBW scrubber (Matheson Gas Products) removed any residual oxygen and moisture. Toluene, hexanes, pentane, and tetrahydrofuran were dried and purified using a Grubbs/Dow solvent purification system and stored in 500 mL thick-walled glass vessels over sodium/benzophenone ketal and distilled under reduced pressure. C₆D₆ was dried over sodium/benzophenone ketal. All dried solvents were degassed, and vacuum distilled prior to use. ¹H and ¹³C NMR spectroscopy chemical shifts were referenced to residual proteo-solvent resonances and naturally abundant ¹³C resonances for all deuterated solvents. Chemical shift assignments are based on ¹H, ¹H{³¹P}, ¹³C{¹H}, ³¹P{¹H}, ¹H-COSY and ¹H-¹³C-HSQC experiments performed on the Ascend-500 or Avance-600 MHz spectrometers. L_H⁶ and L_{NMe₂}⁷ were prepared from literature methods. All other reagents were purchased from Sigma-Aldrich and used as received. Elemental analysis was performed on site by Johnson Li using either a Perkin Elmer Model 2400 Series II analyzer, or an Elementar UNICUBE analyzer. Solution high resolution mass spectrometry analysis was performed by Wade White HRMS on an Agilent 6520 Q-TOF LC-MS system using a syringe pump to introduce the sample. Samples were prepared under an inert argon glovebox atmosphere in a gas-tight syringe. Infrared samples were prepared as KBr pellets, typically at 1% by weight, and infrared spectra were collected on a Nicolet Avatar FT-IR spectrometer.

Synthesis of L_HRuCl₂

To a 100 mL thick-walled glass pressure vessel charged with L_H (0.130 g, 0.295 mmol), [Ru(*p*-cymene)Cl₂]₂ (0.090, 148 mmol) and a Teflon stir bar 10 mL of toluene was added. The flask was sealed, and the solution was stirred at 70°C for 24h. Volatiles were removed under high vacuum and the residue was washed with *n*-pentane (10 mL). An orange-red solid was obtained in 94% yield (0.170 g, 0.277 mmol). X-ray quality crystals were obtained by slow diffusion of *n*-pentane into a solution of L_HRuCl₂ in benzene.

³¹P{¹H} NMR (243 MHz, C₆D₆) δ 42.21 (s).

¹H NMR (600 MHz, C₆D₆) δ 7.27 – 7.19 (m, 4H, Ar-H), 7.16-7.13 (m, 2H, Ar-H), 2.88-2.78 (m, 4H, P-CH(CH₃)₂), 1.35-1.28 (m, 30H, C(CH₃), P-CH(CH₃)₂).

¹³C{¹H} NMR (151 MHz, C₆D₆) δ 271.75 (s, Ru=C) 157.12 (t, *J* = 18.8 Hz, ArC) 139.95 (t, *J* = 13.8 Hz, ArC) 135.62 (t, *J* = 6.4 Hz, ArC), 131.20 (Ar-CH), 129.97 (s, ArCH), 126.62 (Ar-CH), 39.77 (s, C-(CH₃)₂) 31.85 (s, C-(CH₃)₂), 24.35 (t, *J* = 10.7 Hz, P-CH(CH₃)₂), 19.84 (P-CH(CH₃)₂), 18.78 (s, P-CH(CH₃)₂).

HRMS (ESI/Q-TOF) *m/z*: [M]⁺ Calcd for C₂₈H₄₀Cl₂P₂Ru: 610.1026, 612.1026, 575.1337 (M-Cl); Found: 610.1844, 612.1817, 575.1320 (M-Cl)

Synthesis of L_{NMe₂}RuCl₂

To a 100 mL thick walled glass pressure vessel charged with L_{NMe₂} (0.300 g, 0.570 mmol), [Ru(*p*-cymene)Cl₂]₂ (0.171 g, 0.279 mmol) and a Teflon stir bar 10 mL of toluene was added. The flask was sealed, and the solution was stirred at 70°C for 24h. Volatiles were removed under high vacuum and the residue was washed with *n*-pentane (10 mL). A dark red solid was obtained in 66% yield (0.256 g, 0.368

mmol). X-ray quality crystals were obtained by slow diffusion of *n*-pentane into a solution of $\text{L}_{\text{NMe}_2}\text{RuCl}_2$ in benzene.

$^{31}\text{P}\{^1\text{H}\}$ (203 MHz, C_6D_6) δ 43.78 (s).

^1H NMR (500 MHz, C_6D_6) δ 6.90 (m, 2H, ArH), 6.57 (d, $J = 2.3$ Hz, 2H, ArH), 2.99 (m, 4H, P-CH(CH₃)₂), 2.50 (s, 12H, N(CH₃)₂), 1.57 (s, 6H, C(CH₃)₂), 1.50 (m, 24H, P-CH(CH₃)₂).

$^{13}\text{C}\{^1\text{H}\}$ NMR (126 MHz, C_6D_6) δ 272.57 (t, $J = 2.52$ Hz, Ru=C), 149.19 (s, ArC), 149.04 (s, ArC), 148.87 (t, $J = 3.0$ Hz, ArC), 143.52 (t, $J = 13.2$ Hz, ArC), 137.53 (t, $J = 7.3$ Hz, ArC), 115.47 (s, ArCH), 110.46 (s, ArCH), 40.31 (s, C(CH₃)₂), 39.79 (s, N(CH₃)₂), 33.05 (s, C(CH₃)₂), 24.79 (t, $J = 10.1$ Hz, PCH(CH₃)₂), 20.54 (s, PCH(CH₃)₂), 19.42 (t, $J = 2.0$ Hz, PCH(CH₃)₂)

Elemental Anal. Calc. (%) for $\text{C}_{32}\text{H}_{50}\text{Cl}_2\text{N}_2\text{P}_2\text{Ru}$: C, 55.17; H, 7.23; N, 4.02. Found: C, 55.17; H, 7.89; N, 4.08.

Synthesis of $\text{L}_\text{H}\text{Ru}(\text{H})\text{Cl}$

To a 100 mL thick-walled glass pressure vessel charged with L_H (0.300 g, 0.681 mmol), $[\text{Ru}(p\text{-cymene})\text{Cl}_2]_2$ (0.198, 0.323 mmol) and a Teflon stir bar, then toluene (10 mL) and triethylamine (0.5 mL, 3.59 mmol) were added. The flask was sealed, and the solution was stirred at 70°C for 24h. Volatiles were removed under high vacuum and the residue was washed with *n*-pentane (5 mL). The residue was then extracted with toluene (10 mL) and filtered through a 0.2 μm PTFE syringe filter. Volatiles were removed under vacuum to give a red solid in 67% yield (0.250 g, 0.433 mmol). X-ray quality crystals were obtained by slow diffusion of *n*-pentane into a solution of $\text{L}_\text{H}\text{Ru}(\text{H})\text{Cl}$ in cyclohexane.

$^{31}\text{P}\{^1\text{H}\}$ NMR (243 MHz, C_6D_6) δ 64.45.

^1H NMR (600 MHz, C_6D_6) δ 7.34 (t, $J = 7.5$ Hz, 2H, ArH), 3.16 (s, 2H, PCH(CH₃)₂), 2.36 (d, $J = 6.8$ Hz, 2H, PCH(CH₃)₂), 1.38 (s, 3H, C(CH₃)₂), 1.33 (s, 3H, C(CH₃)₂), 1.31 – 1.25 (m, 6H, PCH(CH₃)₂), 1.17 (dt, $J = 12.6$, 5.3 Hz, 12H, PCH(CH₃)₂), 1.05 (q, $J = 7.4$ Hz, 6H, PCH(CH₃)₂), -11.75 (t, $J = 18.8$ Hz, 1H, Ru-H).

^{13}C NMR (151 MHz, C_6D_6) δ 275.2 (t, $J = 5.4$ Hz, Ru=C), 156.9 (t, $J = 19.6$ Hz, ArCH), 141.0 (t, $J = 14.6$ Hz, ArCH), 136.2 (t, $J = 6.6$ Hz, ArCH), 130.1 (ArC), 39.5 (C(CH₃)₂), 32.7 (C(CH₃)₂), 30.0 (C(CH₃)₂), 24.1 (t, $J = 9.7$ Hz, PCH(CH₃)₂), 23.7 (t, $J = 10.6$ Hz, PCH(CH₃)₂), 19.7 (PCH(CH₃)₂), 19.1 (PCH(CH₃)₂), 18.7 (PCH(CH₃)₂), 17.6 (PCH(CH₃)₂)

Missing aromatic signals overlap with benzene. At high concentrations the carbon resonances are seen at 130.0 and 127.2 ppm.

HRMS (ESI/Q-TOF) m/z : $[\text{M}]^+$ Calcd for $\text{C}_{28}\text{H}_{41}\text{ClP}_2\text{Ru}$: 575.1332; Found: 575.1332

Synthesis of $\text{L}_{\text{NMe}_2}\text{Ru}(\text{H})\text{Cl}$:

To a 100 mL thick walled glass pressure vessel charged with L_{NMe_2} (0.300 g, 0.570 mmol), $[\text{Ru}(p\text{-cymene})\text{Cl}_2]_2$ (0.174g, 0.284 mmol) and a Teflon stir bar, then toluene (10 mL) and NEt_3 (0.5 mL, 3.59 mmol) were added. The flask was sealed, and the solution was stirred at 70°C for 24h. Volatiles were removed under high vacuum and the residue was washed with *n*-pentane (5 mL). The residue was then extracted with toluene (10 mL) and filtered through a 0.2 μm PTFE syringe filter. Volatiles were removed

under vacuum to give a dark red solid in 85% yield (0.320 g, 0.483 mmol). X-ray quality crystals were obtained by cooling a saturated toluene solution to -20°C.

$^{31}\text{P}\{^1\text{H}\}$ NMR (203 MHz, C_6D_6) δ 65.43 (s).

^1H NMR (500 MHz, C_6D_6) δ 6.86 (m, 2H, ArH), 6.60 (d, $J = 2.2$ Hz, 2H, ArH), 3.29 (m, 2H, PCH(CH₃)₂), 2.50 (s, 14H, N(CH₃)₂, PCH(CH₃)₂), 1.65 (s, 3H, C(CH₃)₂), 1.60 (s, 3H, C(CH₃)₂), 1.44 (m, 6H, PCH(CH₃)₂), 1.36 (m, 12H, PCH(CH₃)₂), 1.23 (m, 6H, PCH(CH₃)₂), -14.57 (t, $J = 19.4$ Hz, 1H, Ru-H).

Note: one set of the proton resonances for PCH(CH₃)₂ overlapped with the resonance for N(CH₃)₂, this was elucidated ^1H - ^{13}C -HSQC NMR.

$^{13}\text{C}\{^1\text{H}\}$ NMR (126 MHz, C_6D_6) δ 272.49 (t, $J = 5.3$ Hz, Ru=C), 149.50 (t, $J = 2.9$ Hz, ArC), 148.93 (t, $J = 19.8$ Hz, ArC), 143.96 (t, $J = 13.5$ Hz, ArC), 137.78 (t, $J = 7.5$ Hz, ArC), 114.37 (s, ArCH), 110.99 (s, ArCH), 46.85 (s, C(CH₃)₂), 39.93 (N(CH₃)₂), 34.13 (s, C(CH₃)₂), 31.23 (s, C(CH₃)₂), 24.68 (t, $J = 8.7$ Hz, PCH(CH₃)₂), 24.18 (t, $J = 11.0$ Hz, PCH(CH₃)₂), 20.06 (t, PCH(CH₃)₂), 19.48 (t, PCH(CH₃)₂), 18.92 (t, $J = 4.3$ Hz, PCH(CH₃)₂), 17.81 (s, PCH(CH₃)₂).

Elemental Anal. Calc. (%) for $\text{C}_{32}\text{H}_{51}\text{ClN}_2\text{P}_2\text{Ru}$: C, 58.04; H, 7.76; N, 4.23. Found: C, 57.20; H, 8.00; N, 3.98.

Synthesis of $\text{L}_{\text{HH}}\text{Ru}(\text{H})_3/\text{L}_{\text{HH}}\text{RuH}$

A 100 mL round-bottomed flask charged with $\text{L}_{\text{H}}\text{Ru}(\text{H})\text{Cl}$ (0.075g, 0.130 mmol), NaO^tBu (0.030 g, 0.312 mmol), a Teflon stir bar, and benzene (15 mL) was attached to a swivel-frit apparatus with a 100 mL receiving flask. The swivel-frit apparatus was degassed and placed under 1 atm of H_2 at room temperature. Over the course of 2 h the solution changed from red to pale yellow and gave $\text{L}_{\text{HH}}\text{Ru}(\text{H})_3$. Removal of the H_2 headspace resulted in a colour change to green and the formation of $\text{L}_{\text{HH}}\text{RuH}$. Volatiles were removed under high vacuum and the resulting residue was extracted and filtered through the swivel-frit apparatus three times with 20 mL of n-pentane. Removal of pentane under high vacuum gave $\text{L}_{\text{HH}}\text{RuH}$ as a green-yellow solid in ~43% yield (0.030 g isolated, yield estimated based on $\text{L}_{\text{HH}}\text{RuH}$ structure). $\text{L}_{\text{HH}}\text{Ru}(\text{H})_3$ could be returned by placing a solution of $\text{L}_{\text{HH}}\text{RuH}$ under an atmosphere of H_2 .

$^{31}\text{P}\{^1\text{H}\}$ NMR (203 MHz, Toluene- d_8) δ 95.08 (s).

^1H NMR (500 MHz, Toluene- d_8) δ 7.33 (d, $J = 7.1$ Hz, 2H, ArH), 7.15-7.06 (m, overlapping, 4H, ArH), 4.99 (s, 1H, CH-Ru), 2.24 – 2.12 (m, 2H, PCH(CH₃)₂), 2.05-1.97 (m, 2H, PCH(CH₃)₂), 1.70 (s, 3H, C(CH₃)₂), 1.28 (s, 3H, C(CH₃)₂), 1.17-1.05 (m, overlapping q, 12H, PCH(CH₃)₂), 0.93 (q, $J = 6.6$ Hz, 6H, PCH(CH₃)₂), 0.80 (q, $J = 7.0$ Hz, 6H, PCH(CH₃)₂), -7.80 (br s, 3H, Ru-H).

$^{13}\text{C}\{^1\text{H}\}$ NMR (126 MHz, Toluene- d_8) δ 161.4 – 161.0 (m, ArC), 146.2 (ArC), 126.7 (ArCH), 124.9 (ArCH), 124.7 (ArCH), 40.0 (HC-Ru), 38.1 (C(CH₃)₂), 30.5 (t, $J = 10.3$ Hz, PCH(CH₃)₂), 26.0 (t, $J = 14.2$ Hz, PCH(CH₃)₂), 25.6 (C(CH₃)₂), 19.9 (C(CH₃)₂), 18.8 (PHC(CH₃)₂). Missing 1 Ar-C, likely overlapped with toluene- d_8 .

Additional missing 3 PHC(CH₃)₂ signals overlapping with methyl signal from toluene- d_8 , as confirmed by ^1H - ^{13}C HSQC NMR.

Synthesis of $\text{L}_{\text{NMe}_2}\text{Ru}(\text{H})_3/\text{L}_{\text{HNMe}_2}\text{RuH}$:

A 100 mL round-bottomed flask charged with $\text{L}_{\text{NMe}_2}\text{Ru}(\text{H})\text{Cl}$ (0.150 g, 0.227 mmol), NaO^tBu (0.044 g, 0.453 mmol), a Teflon stir bar, and benzene (15 mL) was attached to a swivel-frit apparatus

with a 100 mL receiving flask. The swivel-frit apparatus was degassed and placed under 1 atm of H₂ at room temperature. Over the course of 2 h the solution changed from dark red to pale yellow and gave **L_{NMe₂}Ru(H)₃**. Removal of the H₂ headspace resulted in a colour change to dark green and the formation of **L_{HNMe₂}RuH**. Volatiles were removed under high vacuum and the resulting residue was extracted and filtered through the swivel-frit apparatus three times with 20 mL of *n*-pentane. Removal of pentane under high vacuum gave **L_{HNMe₂}RuH** as a dark green solid in 55% yield (0.0784 g isolated, yield estimated based on **L_{HNMe₂}RuH** structure). **L_{NMe₂}Ru(H)₃** could be returned by placing a solution of **L_{HNMe₂}RuH** under an atmosphere of H₂.

Characterization of **L_{NMe₂}Ru(H)₃**:

³¹P{¹H} (203 MHz, C₆D₆) δ 95.85.

¹H NMR (298 K, 500 MHz, C₆D₆) δ 7.06 (s, 2H, ArH), 6.78 (s, 2H, ArH), 5.00 (s, 1H, HC-Ru), 2.76 (s, 12H, N(CH₃)₂), 2.32 (s, 2H, PCH(CH₃)₂), 2.14 (s, 2H, PCH(CH₃)₂), 1.83 (s, 3H, C(CH₃)₂), 1.50 (s, 3H, C(CH₃)₂), 1.21 (s, 12H, PCH(CH₃)₂), 1.08 (s, 6H, , PCH(CH₃)₂), 1.01 (s, 6H, PCH(CH₃)₂), -7.52 (br s, 3H, Ru-H).

¹³C{¹H} NMR (126 MHz, C₆D₆) δ 151.36 (t, *J* = 18.3 Hz, ArC), 148.98 (t, *J* = 3.5 Hz, ArC), 145.93 (t, *J* = 8.0 Hz, ArC), 138.72 (t, *J* = 19.0 Hz, ArC), 111.67 (s, ArCH), 110.99 (s, ArCH), 67.83 (s, Ru-CH) 41.74 (s, C(CH₃)₂), 40.43 (s, N(CH₃)₂), 35.35 (s, C(CH₃)₂), 35.13 – 34.53 (m, PCH(CH₃)₂), 30.68 – 29.61 (m, PCH(CH₃)₂), 26.23 – 25.31 (m, PCH(CH₃)₂), 25.21 ((s, C(CH₃)₂), 20.14 (m, PCH(CH₃)₂), 18.66 (s, PCH(CH₃)₂).

Characterization of **L_{HNMe₂}RuH**:

³¹P{¹H} (203 MHz, C₆D₆) δ 100.14, 91.80, 90.42, 86.72, 82.79, 81.40, 79.46, 76.16, 72.22, 63.97.

HRMS (ESI/Q-TOF) *m/z*: [M]⁺ Calcd for C₃₂H₅₁N₂P₂Ru 627.2565; Found 627.2574

IR (KBr, 298 K, cm⁻¹): 3063 (w), 2850 (m) 2753 (m), 2120 (w, br, Ru-H), 1938 (w, br, Ru-H).

Synthesis of **L_{DNMe₂}Ru(D)₃**

L_{DNMe₂}Ru(D)₃ was synthesized by placing a sample of **L_{HNMe₂}Ru(H)₃** under an atmosphere of D₂ gas.

Characterization of [**L_{HNMe₂}Ru(H)**](μ-N₂)

³¹P{¹H} (203 MHz, C₆D₆) δ 75.46

IR (KBr, 298 K, cm⁻¹): 3087 (w), 2927 (m), 2792 (w), 2117 (w).

Synthesis of **L_HRu(H)-κ²-O₂CH**

To a 100 mL thick-walled glass pressure vessel charged with **L_{HH}RuH** (0.065 g, 0.121 mmol) and a Teflon stir bar benzene (10 mL) was added. The vessel was degassed and placed under 1 atmosphere of CO₂. An immediate colour change from yellow to red was observed. Initially a mixture of **L_{HH}Ru-κ²-O₂CH** and **L_HRu(H)-κ²-O₂CH** was obtained, with full conversion to **L_HRu(H)-κ²-O₂CH** occurring over 15 minutes at room temperature. Volatiles were removed under high vacuum and an orange-red powder was isolated in 92% yield (0.065 g, 0.111 mmol). Note the yield was based on the **L_{HH}RuH** structure for the starting material.

³¹P{¹H} (203 MHz, C₆D₆) δ 65.36.

^1H NMR (500 MHz, C_6D_6) δ 8.64 (s, 1H, OCHO), 7.33 (t, $J = 7.5$ Hz, 2H, ArH), 7.23 – 7.18 (m, 4H,), 2.62 – 2.51 (m, 2H, PCH(CH_3) $_2$), 2.40 – 2.28 (m, 2H, PCH(CH_3) $_2$), 1.42 (s, 3H, C(CH_3)), 1.36 (p, $J = 7.3$ Hz, 6H, PCH(CH_3) $_2$), 1.30 (s, 3H, C(CH_3)), 1.18 (q, $J = 7.5, 7.0$ Hz, 12H, PCH(CH_3) $_2$), 1.12 (q, $J = 7.1$ Hz, 6H, PCH(CH_3) $_2$), -8.99 (t, 1H, Ru-H).

^{13}C NMR (126 MHz, C_6D_6) δ 275.59 (Ru=C), 170.86 (s, OCHO), 155.58 (t, $J = 20.3$ Hz, ArC), 140.24 (t, $J = 16.7$ Hz, ArC), 134.77 (t, $J = 7.0$ Hz, ArC), 128.89 (ArCH), 125.88 (ArCH), 124.75 (ArC), 38.23 (CCH $_3$), 32.81 (CCH $_3$), 28.47 (CCH $_3$), 24.02 – 23.46 (m, PCH(CH_3) $_2$), 18.78 (m, PCH(CH_3) $_2$), 18.15 – 17.64 (m, PCH(CH_3) $_2$), 16.87 (m, PCH(CH_3) $_2$).

HRMS (ESI/Q-TOF) m/z : [M] Calcd for $\text{C}_{29}\text{H}_{42}\text{O}_2\text{P}_2\text{Ru}$: 542.1805 (M-CO $_2$); Found: 542.1813 (M-CO $_2$)

Synthesis of $\text{L}_\text{H}\text{Ru}(\text{H})-\kappa^2\text{-O}_2^{13}\text{CH}$:

In a 100 mL thick-walled glass pressure vessel charged with $\text{L}_{\text{NMe}_2}\text{Ru}(\text{H})\text{Cl}$ (0.040 g, 0.069 mmol), ^{13}C -labelled sodium formate (0.010 g, 0.144 mmol) and a Teflon stir bar, 5 mL of benzene was added. The flask was sealed and heated at 75 °C for 2 days. The solution was then cooled and filtered through a 0.2 μm PTFE syringe filter. Volatiles were then removed under high vacuum and a dark red solid was isolated in 84% yield (0.034 g, 0.058 mmol).

^1H NMR (500 MHz, C_6D_6) δ 8.64 (d, $J = 196.1$ Hz 1H, OCHO)

$^{13}\text{C}\{^1\text{H}\}$ NMR (126 MHz, C_6D_6) δ 170.86 (OCHO)

Synthesis of $\text{L}_{\text{NMe}_2}\text{Ru}(\text{H})-\kappa^2\text{-O}_2\text{CH}$:

To a 100 mL thick-walled glass pressure vessel charged with $\text{L}_{\text{HNMe}_2}\text{RuH}$ (0.114 g, 0.182 mmol) and a Teflon stir bar benzene (10 mL) was added. The vessel was degassed and placed under 1 atmosphere of CO $_2$. An immediate colour change from green to red was observed. Volatiles were removed under high vacuum and a dark red powder was isolated in 90% yield (0.110 g, 0.164 mmol) based on the assigned $\text{L}_{\text{HNMe}_2}\text{RuH}$ structure for the starting material.

$^{31}\text{P}\{^1\text{H}\}$ (203 MHz, C_6D_6) δ 67.25.

^1H NMR (500 MHz, C_6D_6) δ 8.77 (s, 1H, OCHO), 6.85 (m, 2H, ArH), 6.62 (d, $J = 2.4$ Hz, 2H, ArH), 2.69 (m, 2H, PCH(CH_3) $_2$), 2.51 (s, 12H, N(CH_3) $_2$), 2.47 – 2.41 (m, 2H, PCH(CH_3) $_2$), 1.63 (s, 3H, C(CH_3)), 1.54 (s, 3H, C(CH_3)), 1.47 (q, $J = 7.3$ Hz, 6H, PCH(CH_3) $_2$), 1.33 (p, $J = 7.4, 6.6$ Hz, 12H, PCH(CH_3) $_2$), 1.26 (q, $J = 7.1$ Hz, 6H, PCH(CH_3) $_2$), -11.14 (t, $J = 19.3$ Hz, 1H, Ru-H)

$^{13}\text{C}\{^1\text{H}\}$ NMR (126 MHz, C_6D_6) δ 274.45 (t, $J = 5.8$ Hz, Ru=C), 170.36 (OCHO), 149.45 (t, $J = 2.9$ Hz, ArC), 148.66 (t, $J = 20.3$ Hz, ArC), 144.24 (t, $J = 14.5$ Hz, ArC), 137.24 (t, $J = 7.7$ Hz, ArC), 113.93 (s, ArCH), 111.18 (ArCH), 40.05 (N(CH_3) $_2$), 39.80 (s, C(CH_3) $_2$), 34.82 (s, C(CH_3) $_2$), 31.31 (s, C(CH_3) $_2$), 30.49 (s, PCH(CH_3) $_2$), 25.39 (m, PCH(CH_3) $_2$), 20.29 – 19.73 (m, PCH(CH_3) $_2$), 19.19 (t, $J = 3.9$ Hz, PCH(CH_3) $_2$), 18.16 (s, PCH(CH_3) $_2$).

Elemental Anal. Calc. (%) for $\text{C}_{33}\text{H}_{52}\text{N}_2\text{O}_2\text{P}_2\text{Ru}$: C, 59.00; H, 7.80; N, 4.17. Found: C, 57.66; H, 7.92; N, 3.77.

HRMS (ESI/Q-TOF) m/z : [M] Calcd for $\text{C}_{33}\text{H}_{52}\text{O}_2\text{P}_2\text{Ru}$: 627.2571 (M $^+$ -CO $_2$); Found: 627.25869 (M $^+$ -CO $_2$)

Note: ^{13}C resonance for OCHO was verified using a ^{13}C -labelled formate sample.

IR (KBr, 298 K, cm^{-1}): 3139w, 2996m, 2139w (Ru-H). C-O stretches were not observed despite ^{13}C labelling, they are expected to overlap with several ligand stretches.

Synthesis of $\text{L}_{\text{NMe}_2}\text{Ru}(\text{H})-\kappa^2\text{-O}_2^{13}\text{CH}$:

In a 100 mL thick-walled glass pressure vessel charged with $\text{L}_{\text{NMe}_2}\text{Ru}(\text{H})\text{Cl}$ (0.030 g, 0.045 mmol), ^{13}C -labelled sodium formate (0.008 g, 0.12 mmol) and a Teflon stir bar 5 mL of benzene was added. The flask was sealed and heated at 75 °C for 2 days. The solution was then cooled and filtered through a 0.2 μm PTFE syringe filter. Volatiles were then removed under high vacuum and a dark red solid was isolated in 92% yield (0.028 g, 0.042 mmol). $\text{L}_{\text{NMe}_2}\text{Ru}(\text{H})-\kappa^2\text{-O}_2^{13}\text{CH}$ could also be prepared by a procedure analogous to $\text{L}_{\text{NMe}_2}\text{Ru}(\text{H})-\kappa^2\text{-O}_2\text{CH}$ using $^{13}\text{CO}_2$.

^1H NMR (500 MHz, C_6D_6) δ 8.77 (d, $J = 193.8$ Hz 1H, OCHO)

$^{13}\text{C}\{^1\text{H}\}$ NMR (126 MHz, C_6D_6) δ 170.36 (OCHO)

NMR Spectra

$^{31}\text{P}\{^1\text{H}\}$, ^1H and $^{13}\text{C}\{^1\text{H}\}$ NMR for Characterization of Reported L_H Supported Compounds

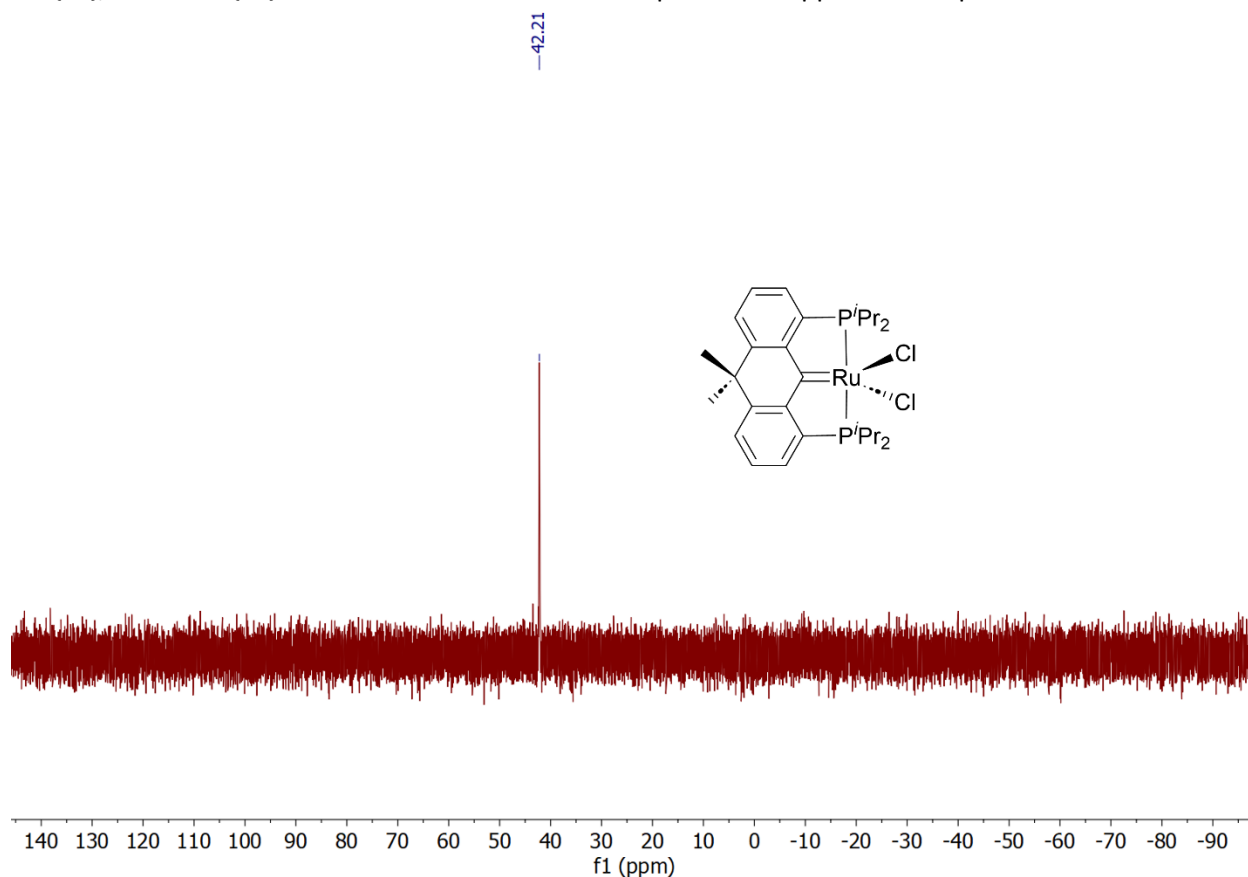


Figure S8: $^{31}\text{P}\{^1\text{H}\}$ spectrum of $\text{L}_\text{H}\text{RuCl}_2$ in C_6D_6 .

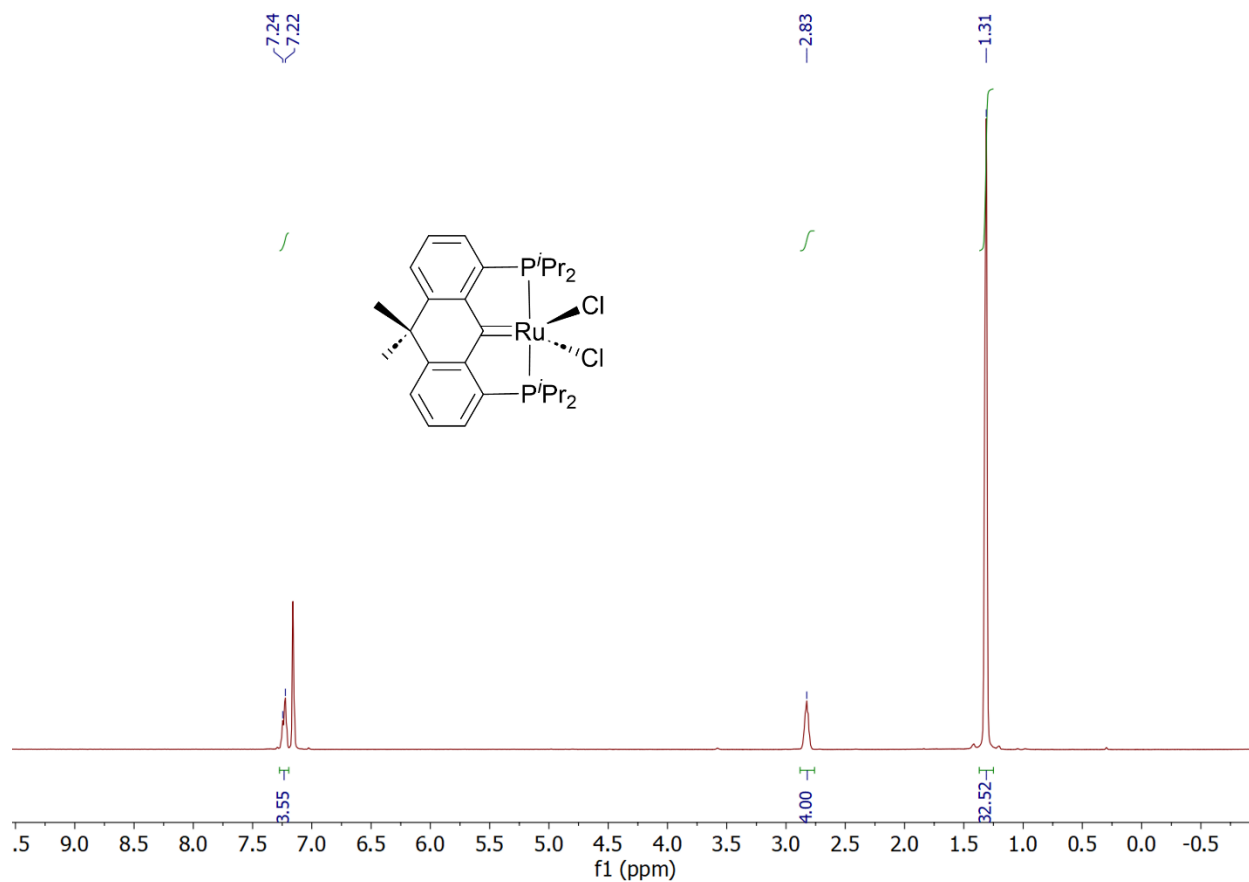


Figure S9: ^1H NMR spectrum of $\text{L}_\text{H}\text{RuCl}_2$ in C_6D_6 . Note all ligand methyl groups overlap at 1.31 ppm and 1 set of aromatic protons overlap with the residual C_6D_6 resonance while the remaining 2 sets of aromatic protons overlap with one another. ^1H - ^1H COSY and ^1H - ^{13}C HSQC used to assign spectra.

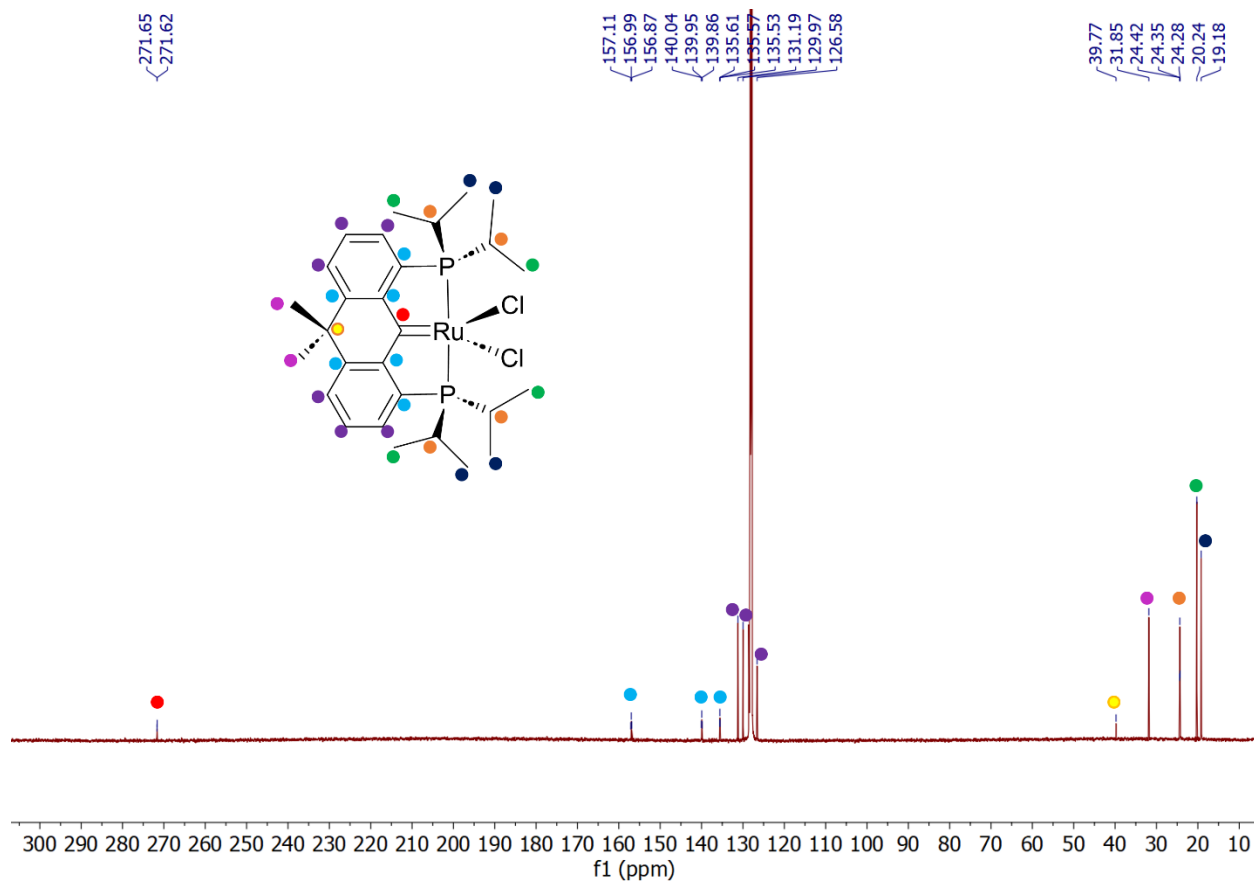


Figure S10: Assigned $^{13}C\{^1H\}$ NMR spectrum of L_HRuCl_2 in C_6D_6 .

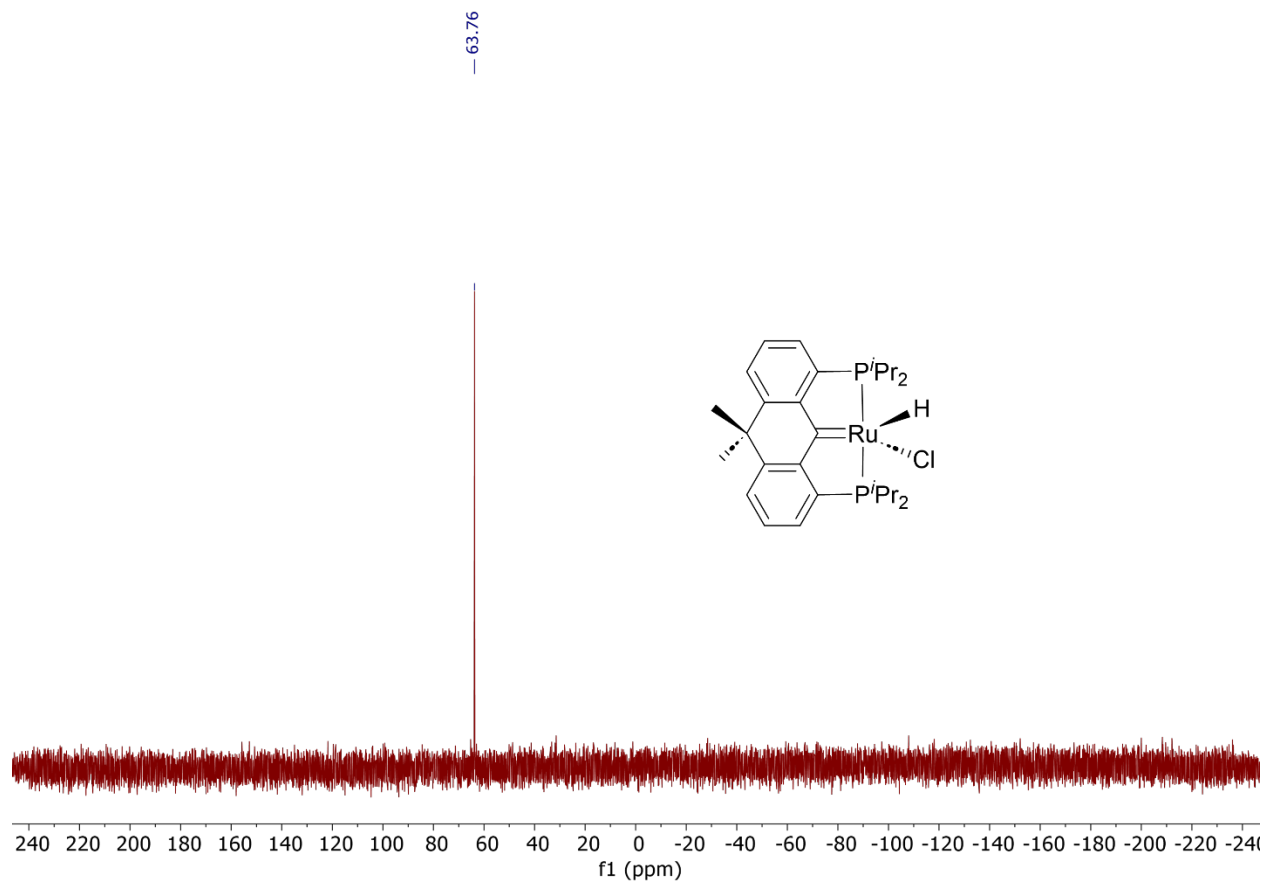


Figure S11: $^{31}\text{P}\{^1\text{H}\}$ spectrum for $\text{L}_\text{H}\text{Ru}(\text{H})\text{Cl}$ in C_6D_6 .

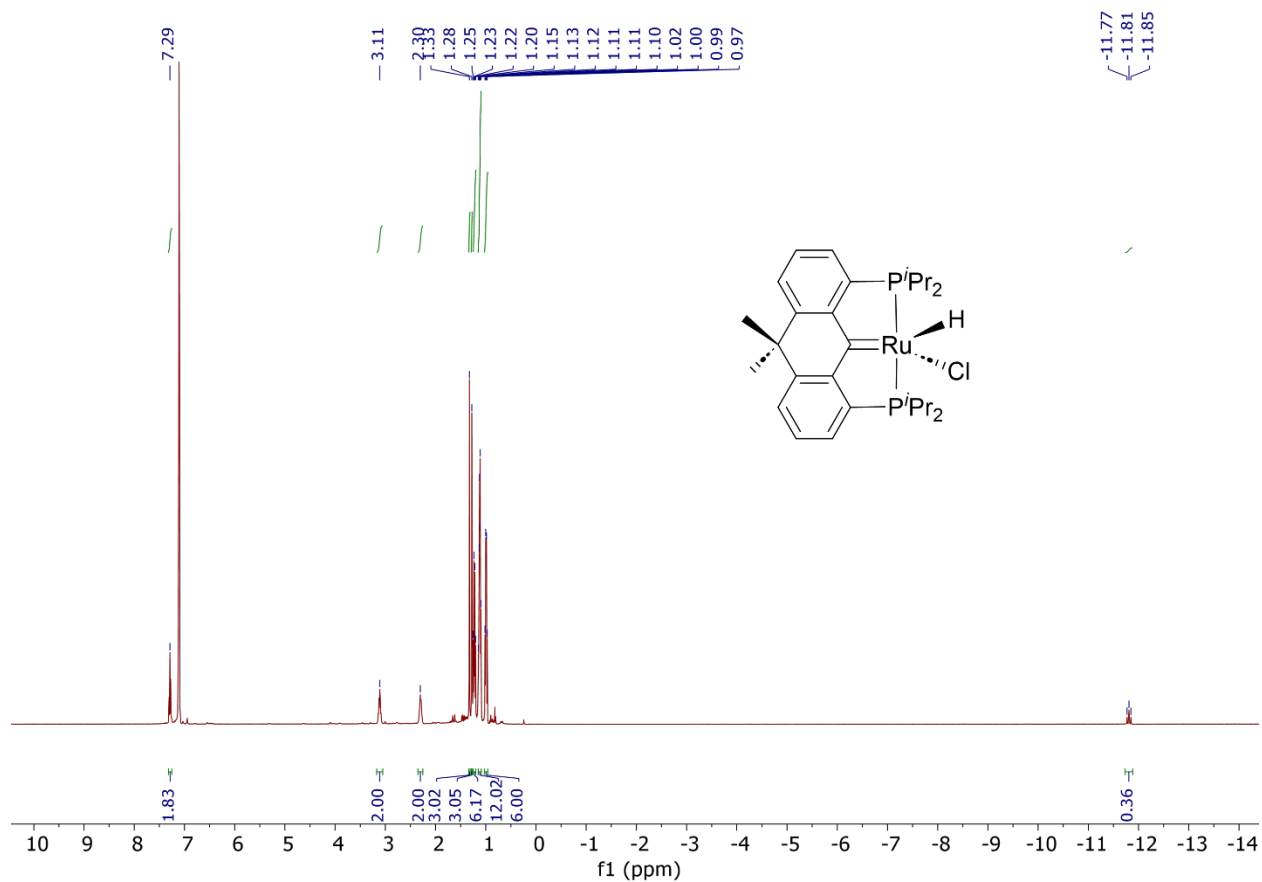


Figure S12: 1H spectrum for $L_H Ru(H)Cl$ in C_6D_6 . Note: missing aromatic resonances overlap with residual benzene resonances from C_6D_6 .

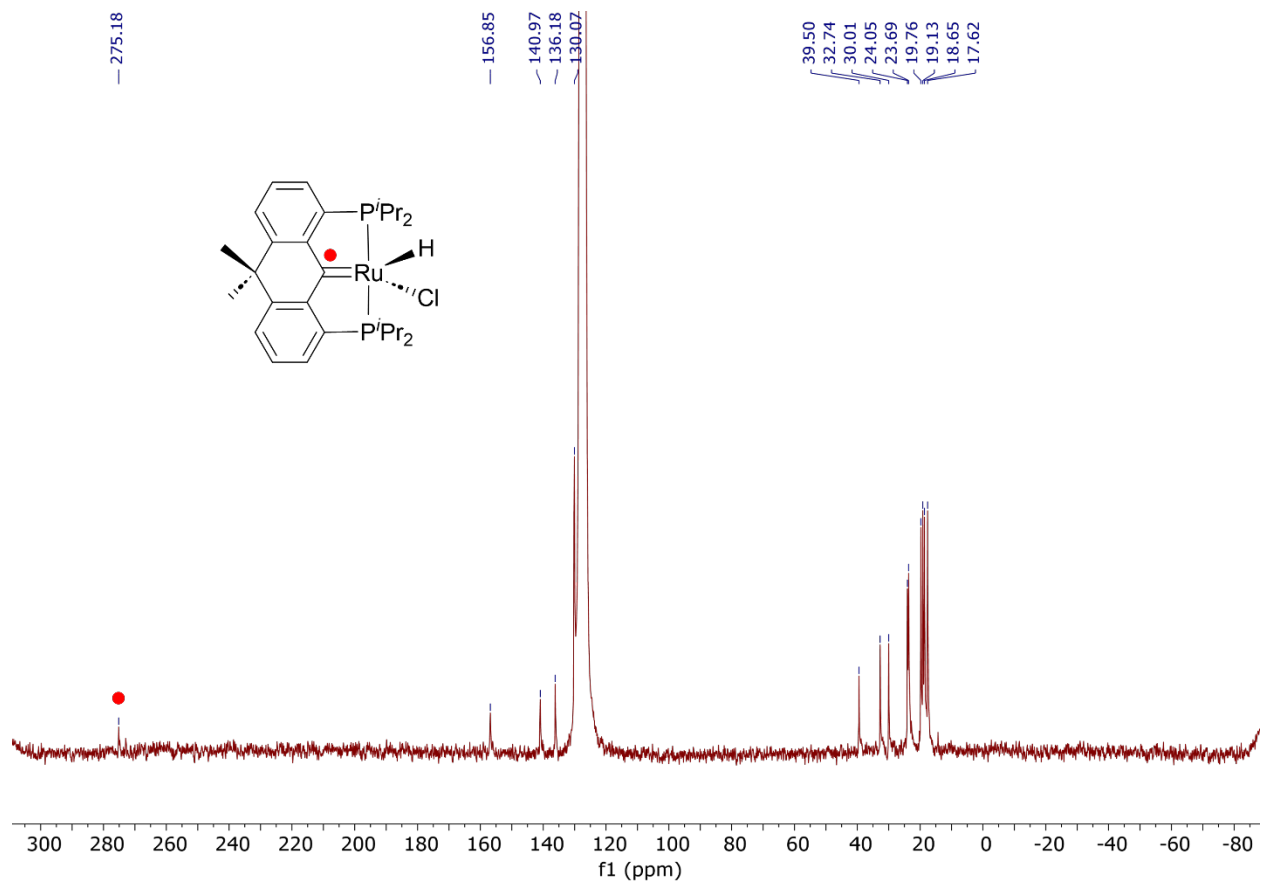


Figure S13: $^{13}C\{^1H\}$ spectrum for $LHRu(H)Cl$ in C_6D_6 . Note: missing aromatic resonances overlap with residual benzene resonances from C_6D_6 .

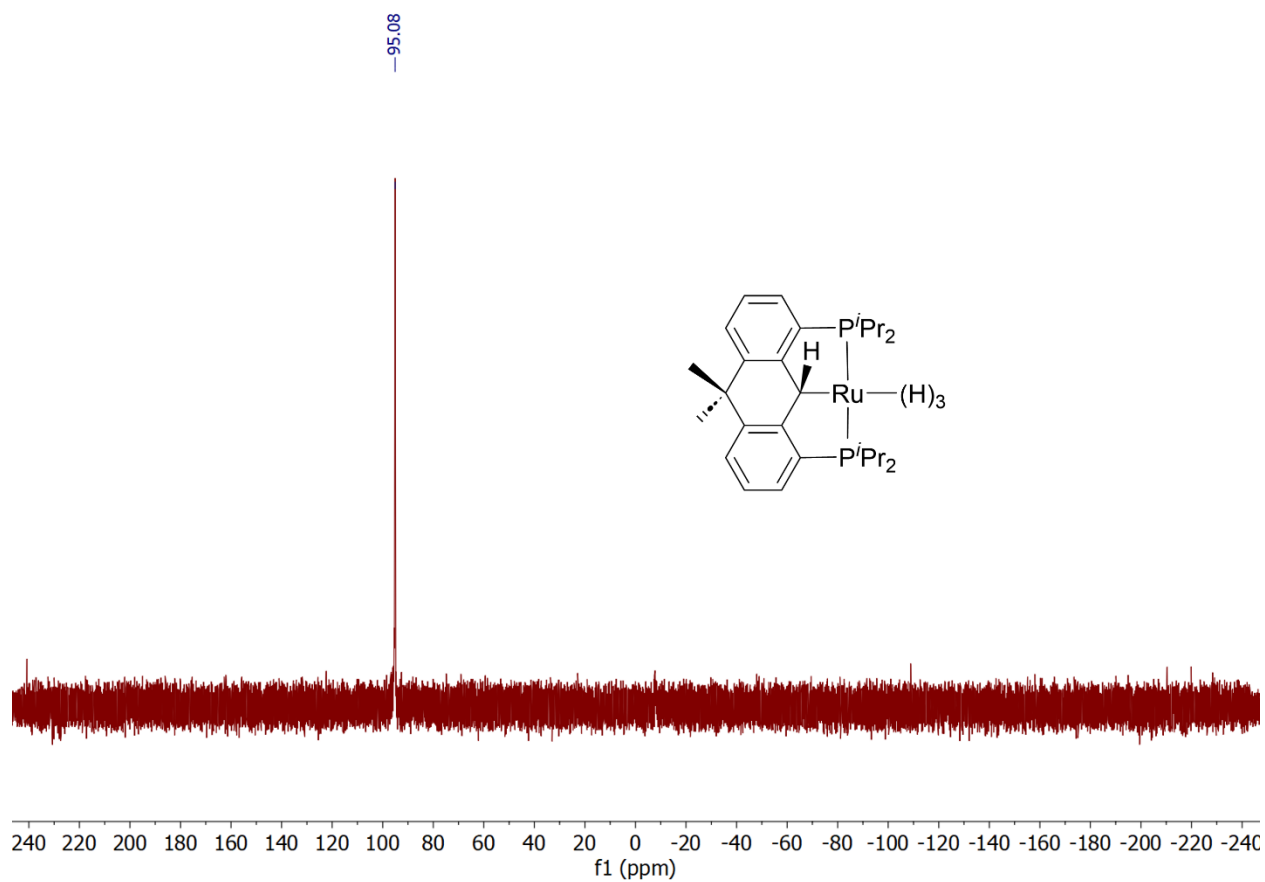


Figure S14: $^{31}\text{P}\{^1\text{H}\}$ NMR spectrum of $\text{L}_{\text{HH}}\text{Ru}(\text{H})_3$ in $\text{toluene-}d_8$, under 1 atm of H_2 .

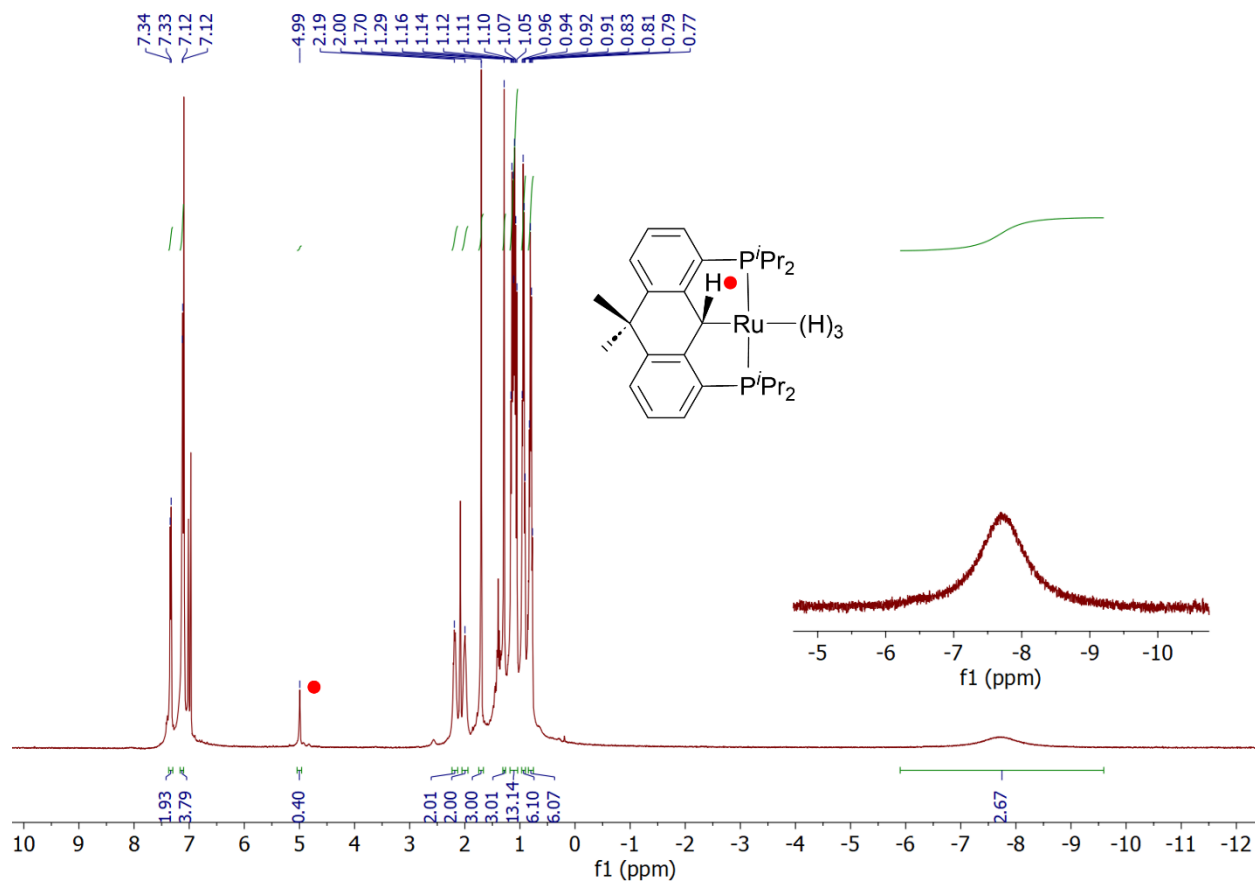


Figure S15: 1H NMR spectrum of $L_{HH}Ru(H)_3$ in toluene- d_8 , under 1 atm of H_2 .

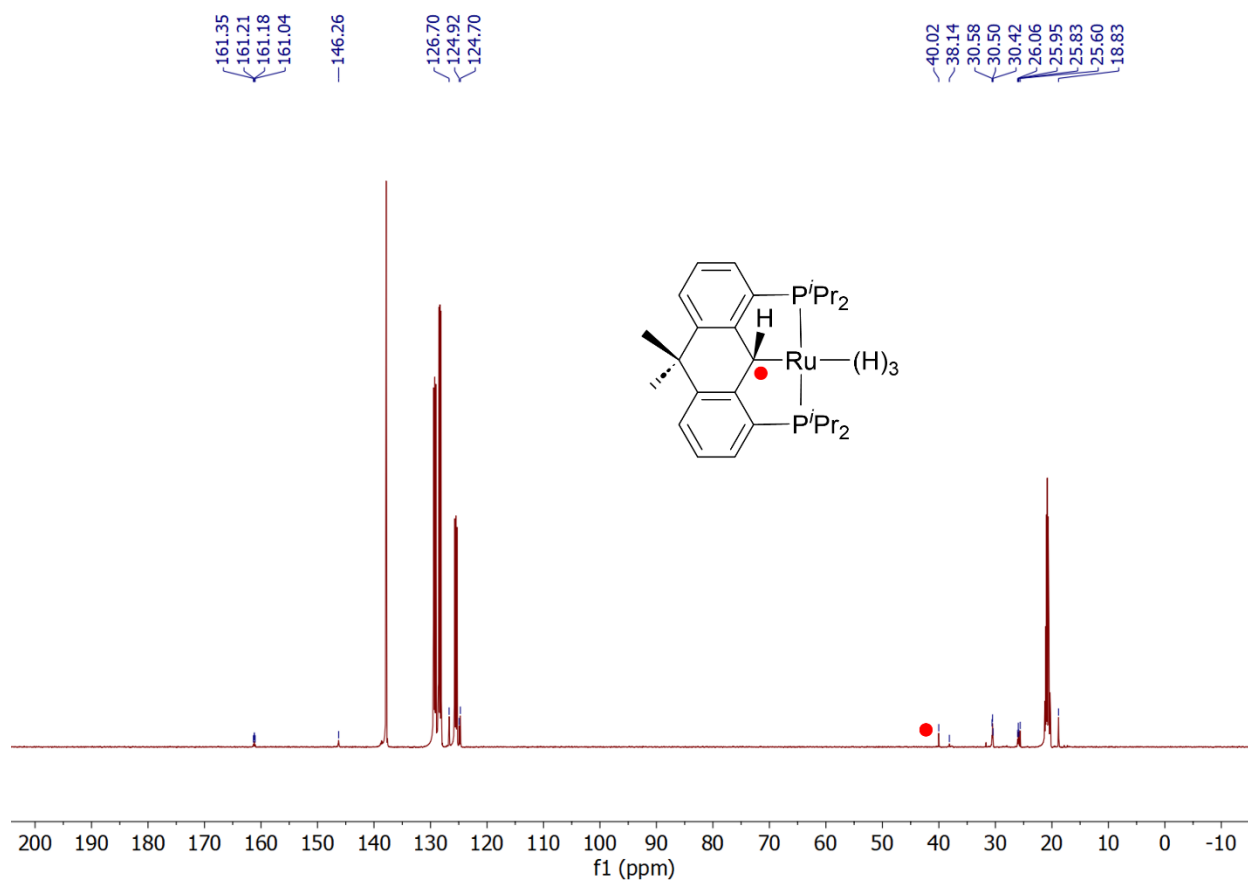


Figure S16: $^{13}\text{C}\{^1\text{H}\}$ NMR spectrum of $\text{L}_{\text{HH}}\text{Ru}(\text{H})_3$ in $\text{toluene-}d_8$, under 1 atm of H_2 .

104.50
98.36
95.02
87.91

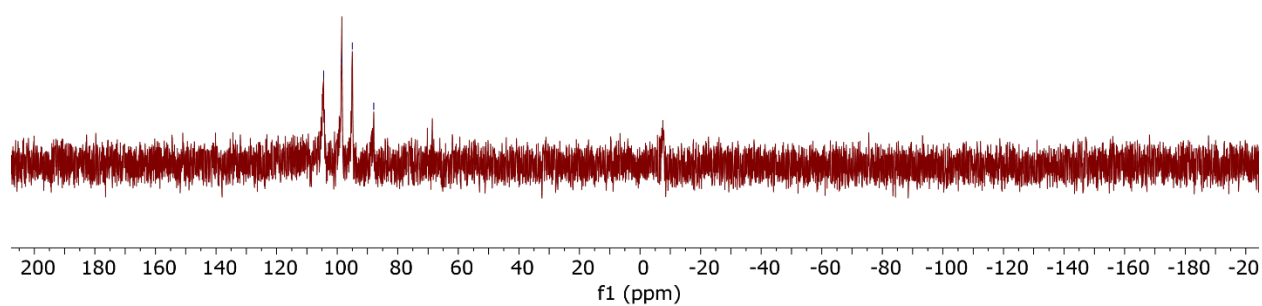
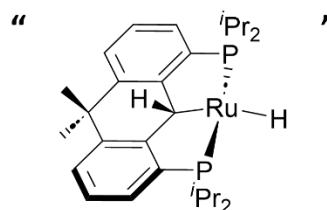


Figure S17: $^{31}\text{P}\{^1\text{H}\}$ NMR spectrum of “ $\text{L}_{\text{HH}}\text{RuH}$ ” in C_6D_6 , under argon. Note: adding 1 atm of H_2 returns $\text{L}_{\text{HH}}\text{Ru}(\text{H})_3$ (Figure S14).

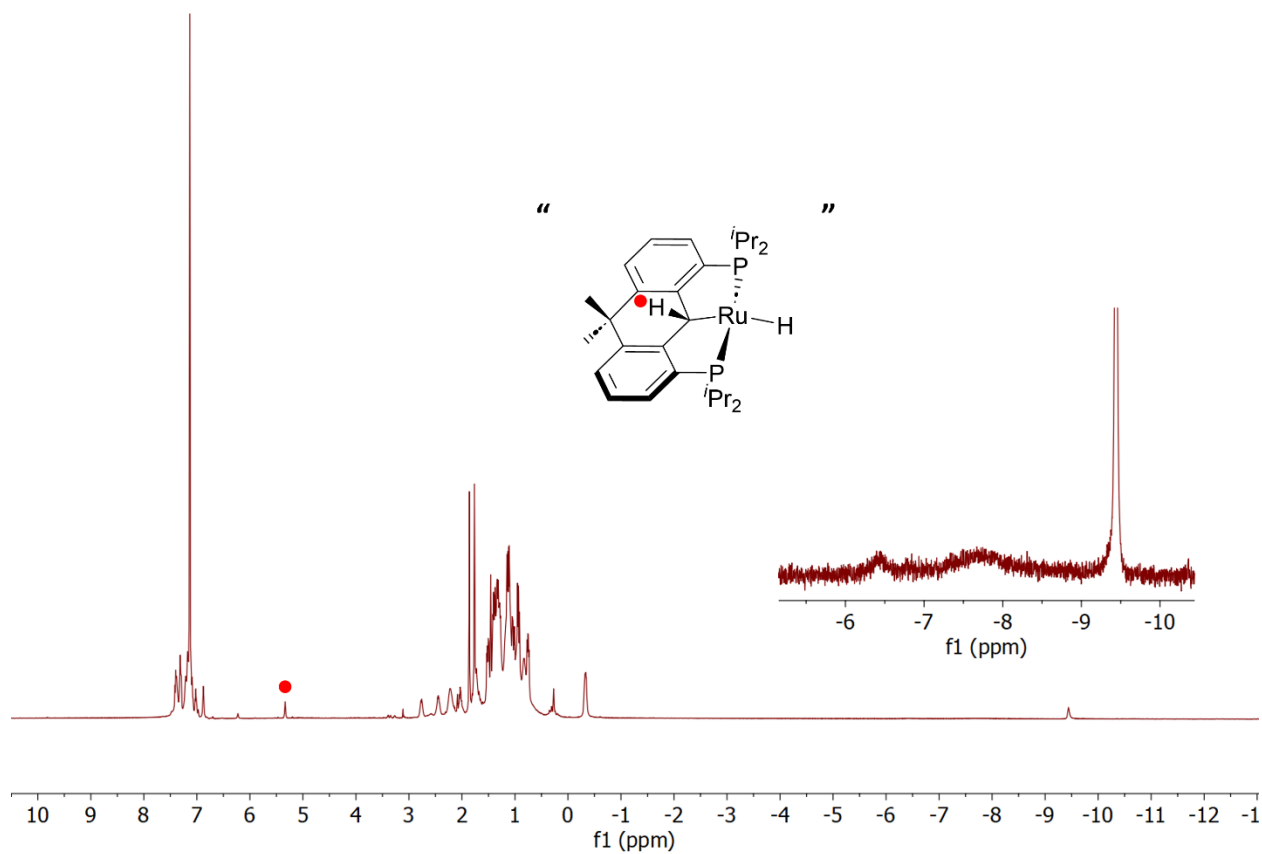


Figure S18: ^1H NMR spectrum of $\text{L}_{\text{HH}}\text{RuH}$ in C_6D_6 , under argon. Note: adding 1 atm of H_2 returns $\text{L}_{\text{HH}}\text{Ru}(\text{H})_3$ (Figure S15).

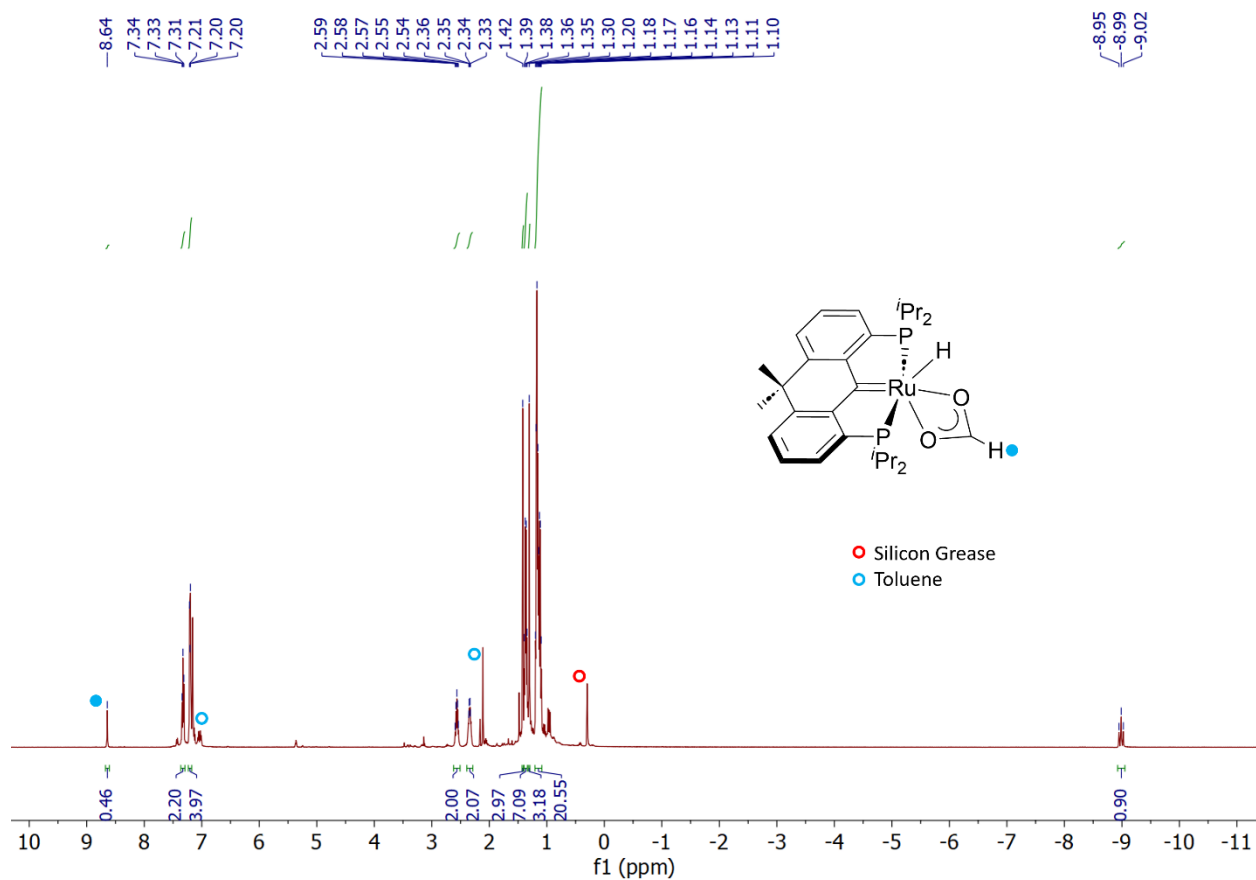


Figure S20: 1H NMR spectrum of $L_{HRu}(H)-\kappa^2-O_2CH$ in C_6D_6 .

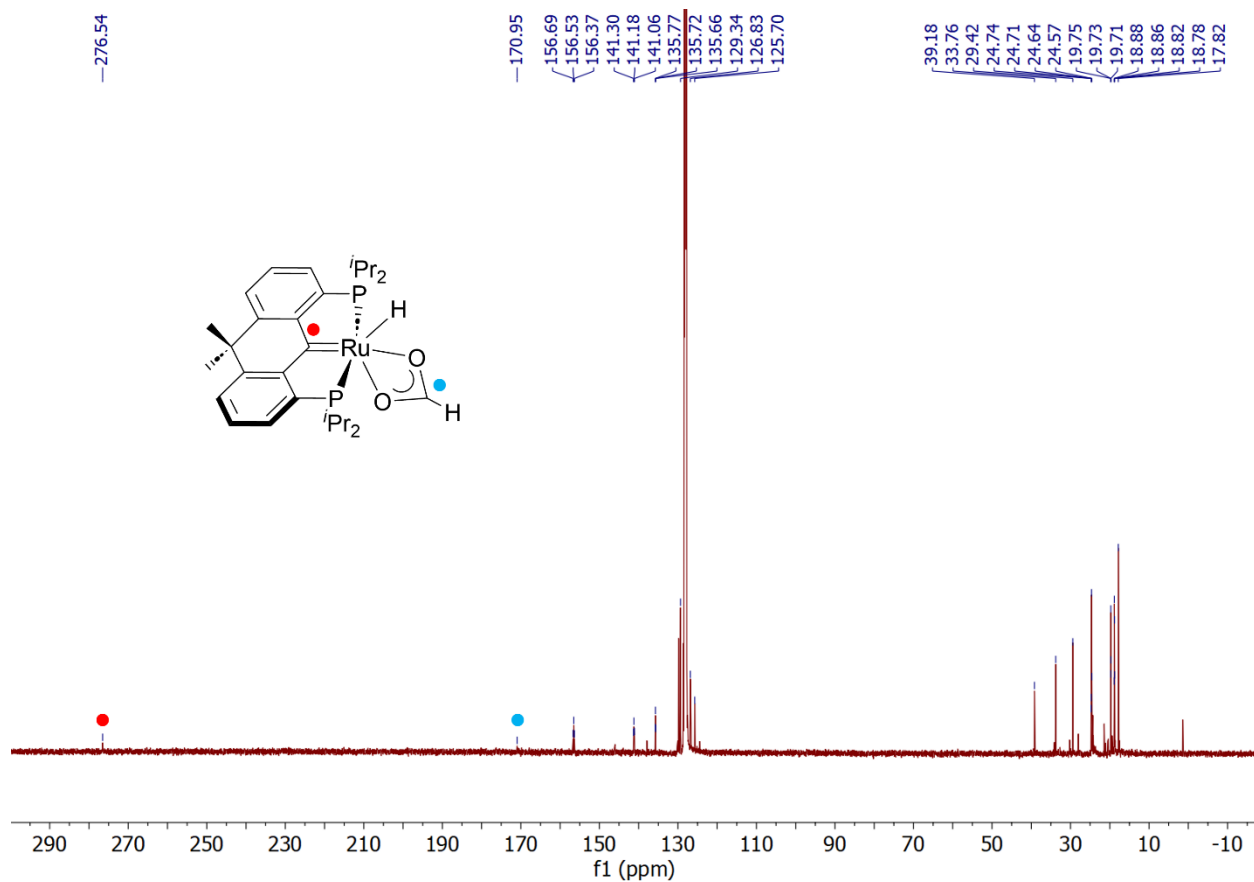


Figure S21: $^{13}C\{^1H\}$ NMR spectrum of $L_{HRu}(H)-\kappa^2-O_2CH$ in C_6D_6 .

$^{31}\text{P}\{^1\text{H}\}$, ^1H and $^{13}\text{C}\{^1\text{H}\}$ NMR for Characterization of Reported L_{NMe_2} Supported Compounds

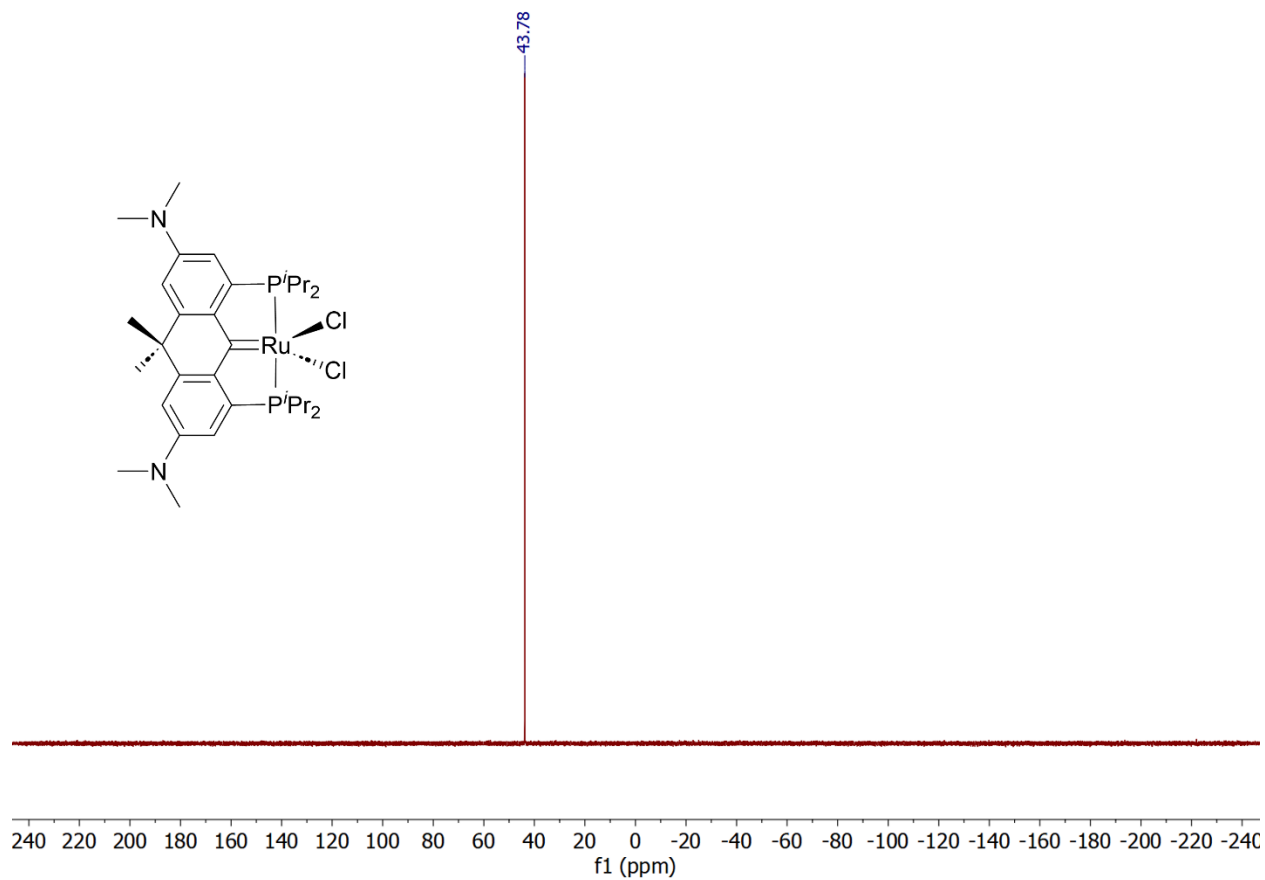


Figure S22: $^{31}\text{P}\{^1\text{H}\}$ NMR spectrum of $\text{L}_{\text{NMe}_2}\text{RuCl}_2$ in C_6D_6 .

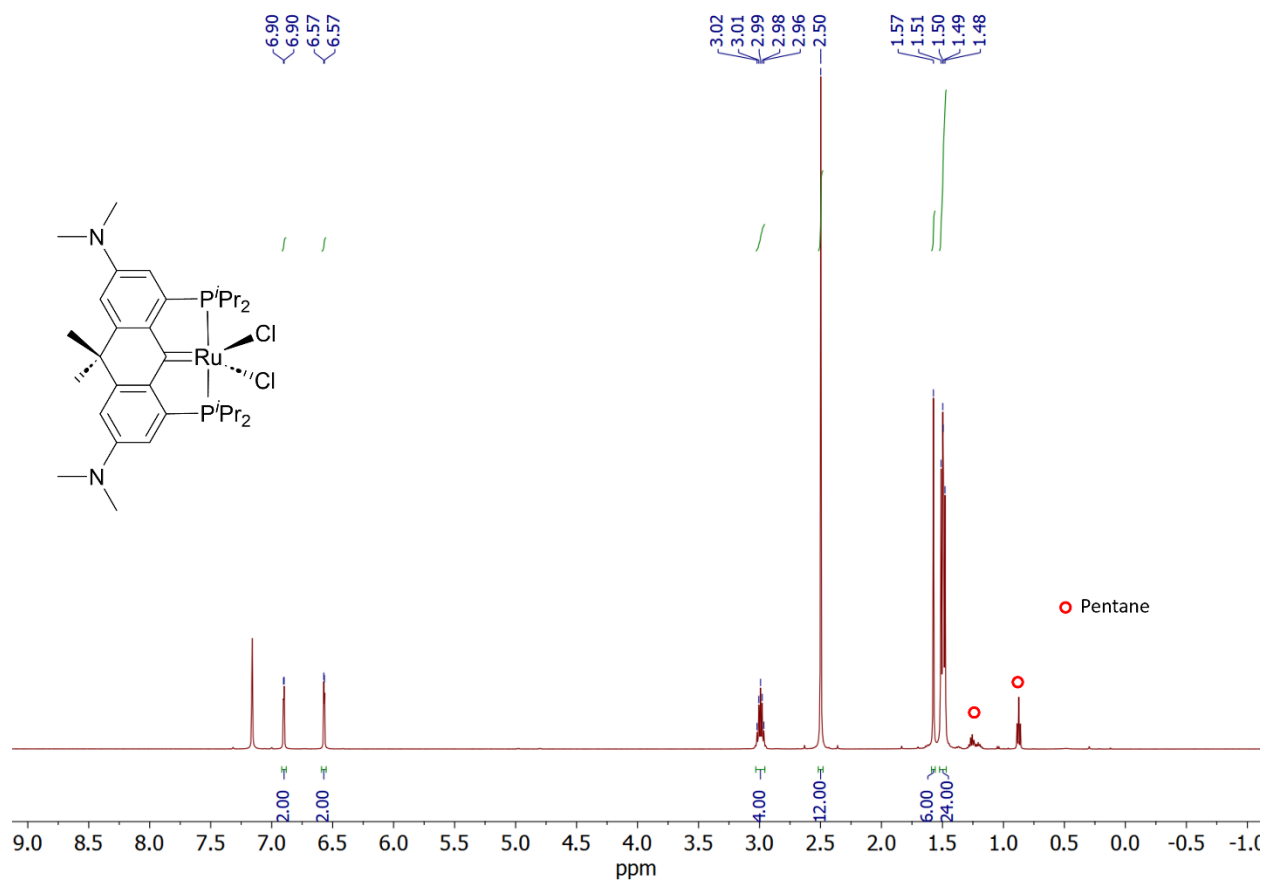


Figure S23: ¹H NMR spectrum of $L_{NMe_2}RuCl_2$ in C_6D_6 .

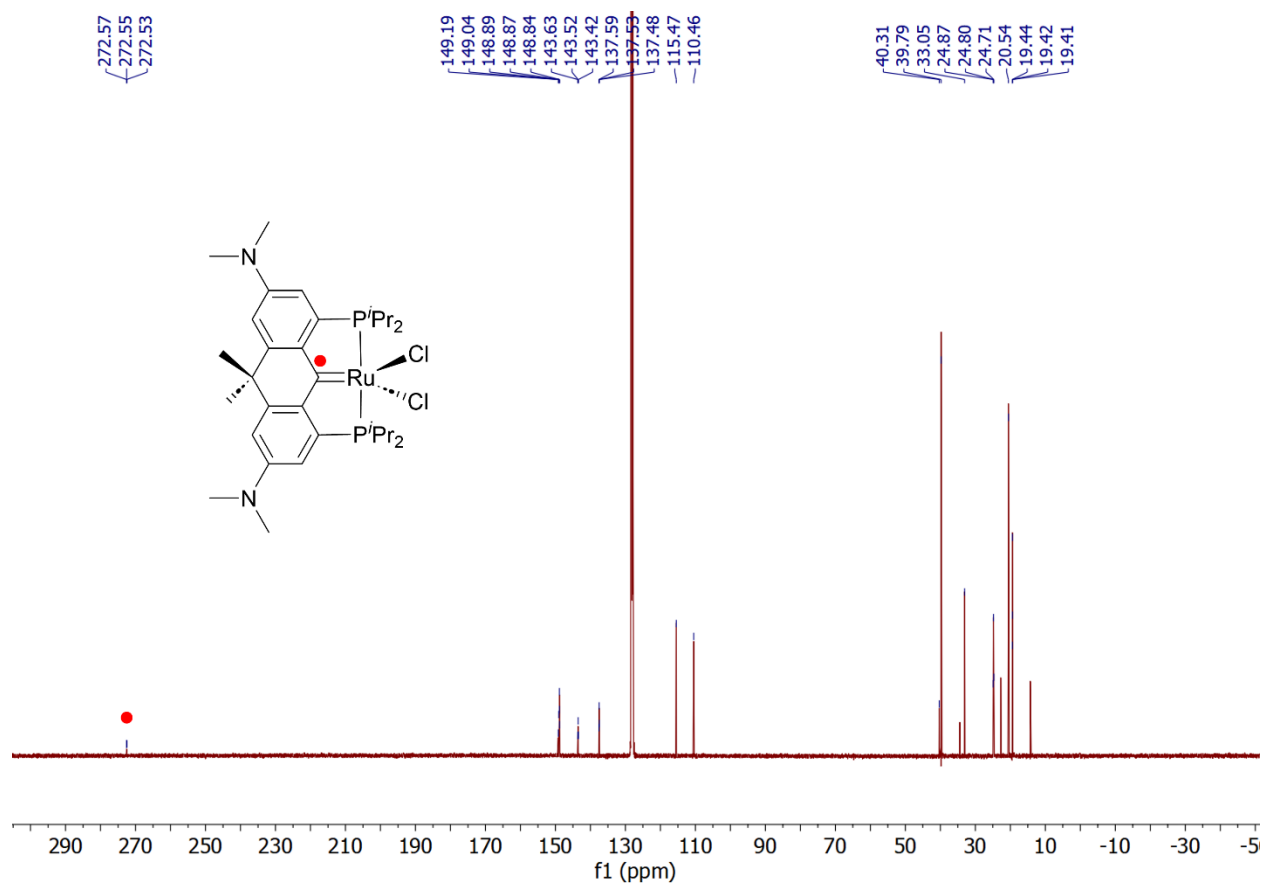


Figure S24: $^{13}C\{^1H\}$ NMR spectrum for $L_{NMe_2}RuCl_2$ in C_6D_6 .

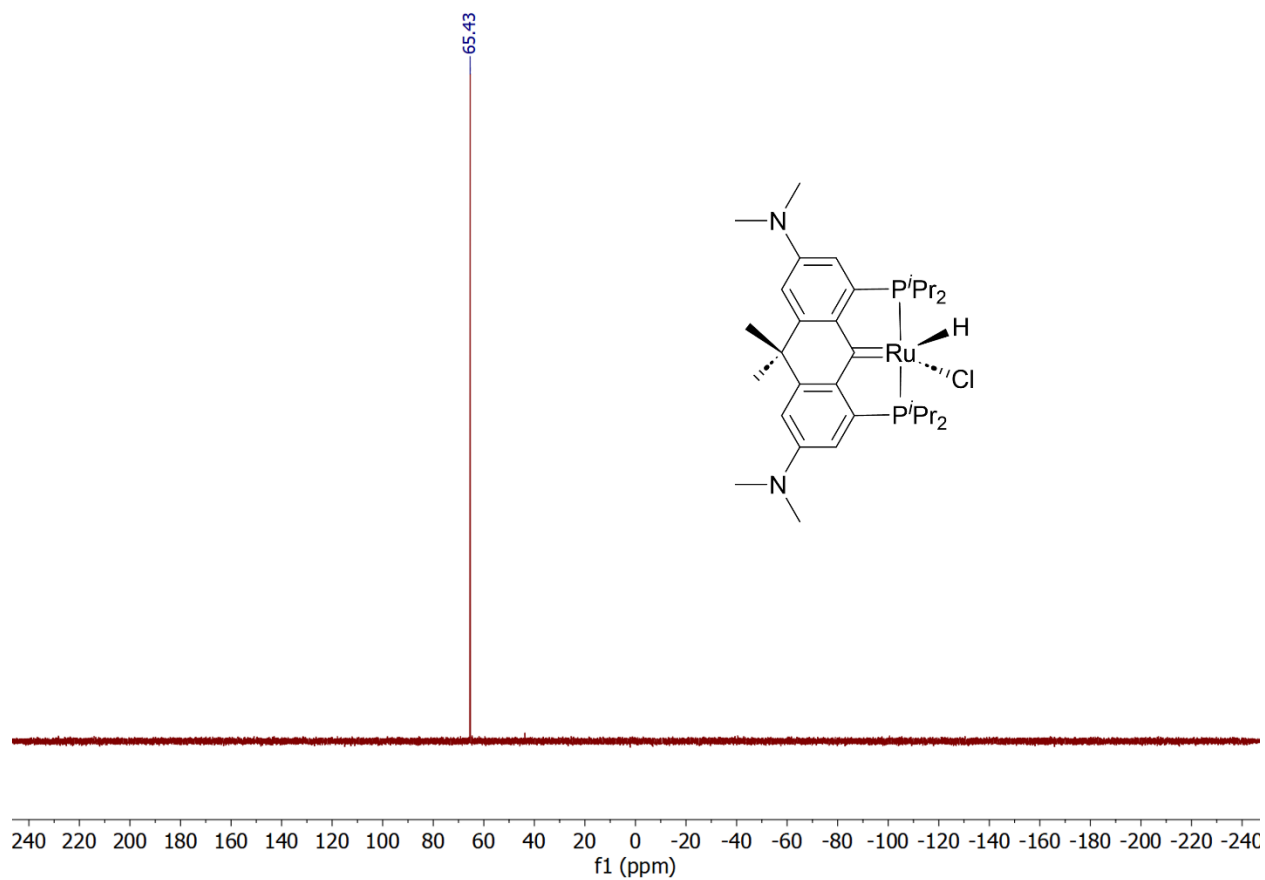


Figure S25: $^{31}\text{P}\{^1\text{H}\}$ NMR spectrum of $\text{L}_{\text{NMe}_2}\text{Ru}(\text{H})\text{Cl}$ in C_6D_6

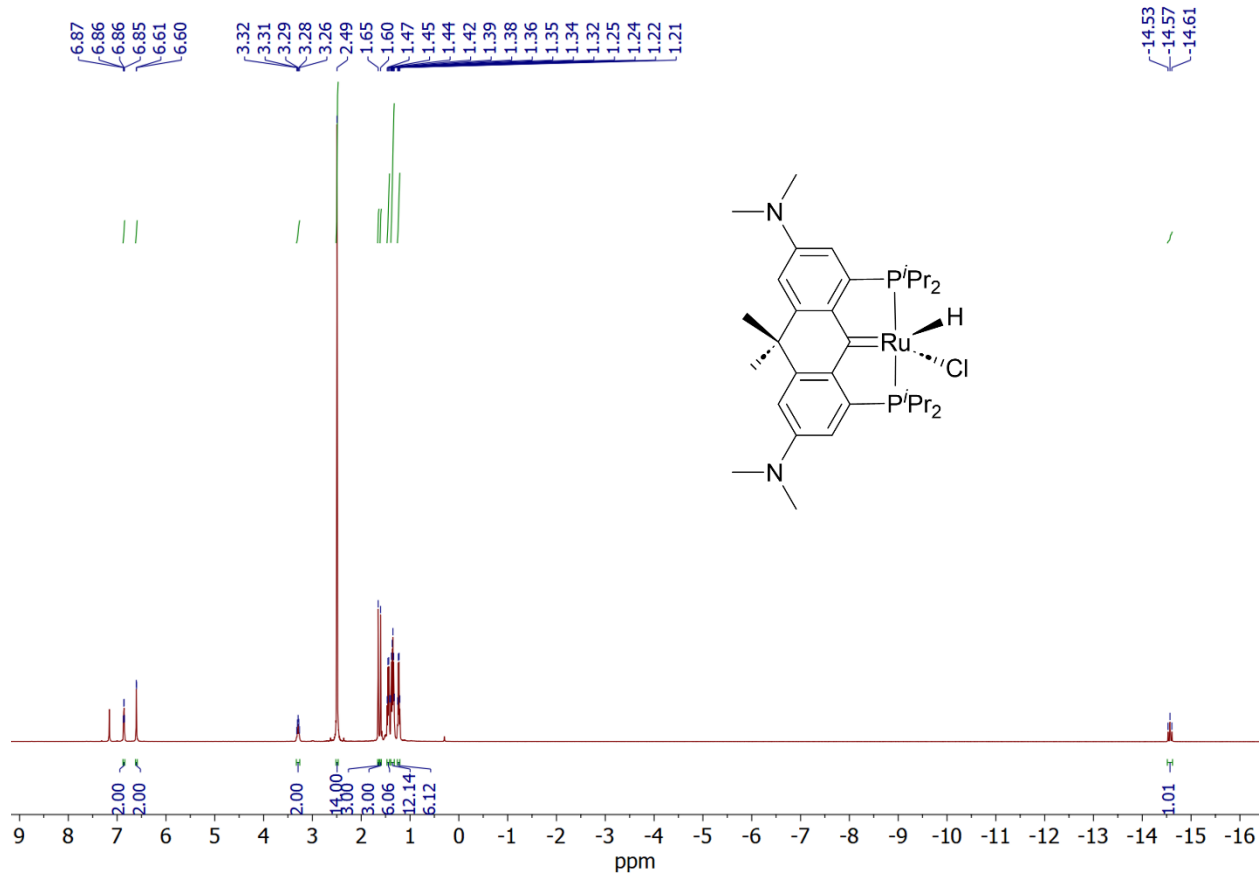


Figure S26: ^1H NMR spectrum of $\text{L}_{\text{NMe}_2}\text{Ru}(\text{H})\text{Cl}$ in C_6D_6 . Note: one set of the proton resonances for $\text{PCH}(\text{CH}_3)_2$ overlapped with the resonance for $\text{N}(\text{CH}_3)_2$, this was verified with ^1H - ^{13}C -HSQC NMR.

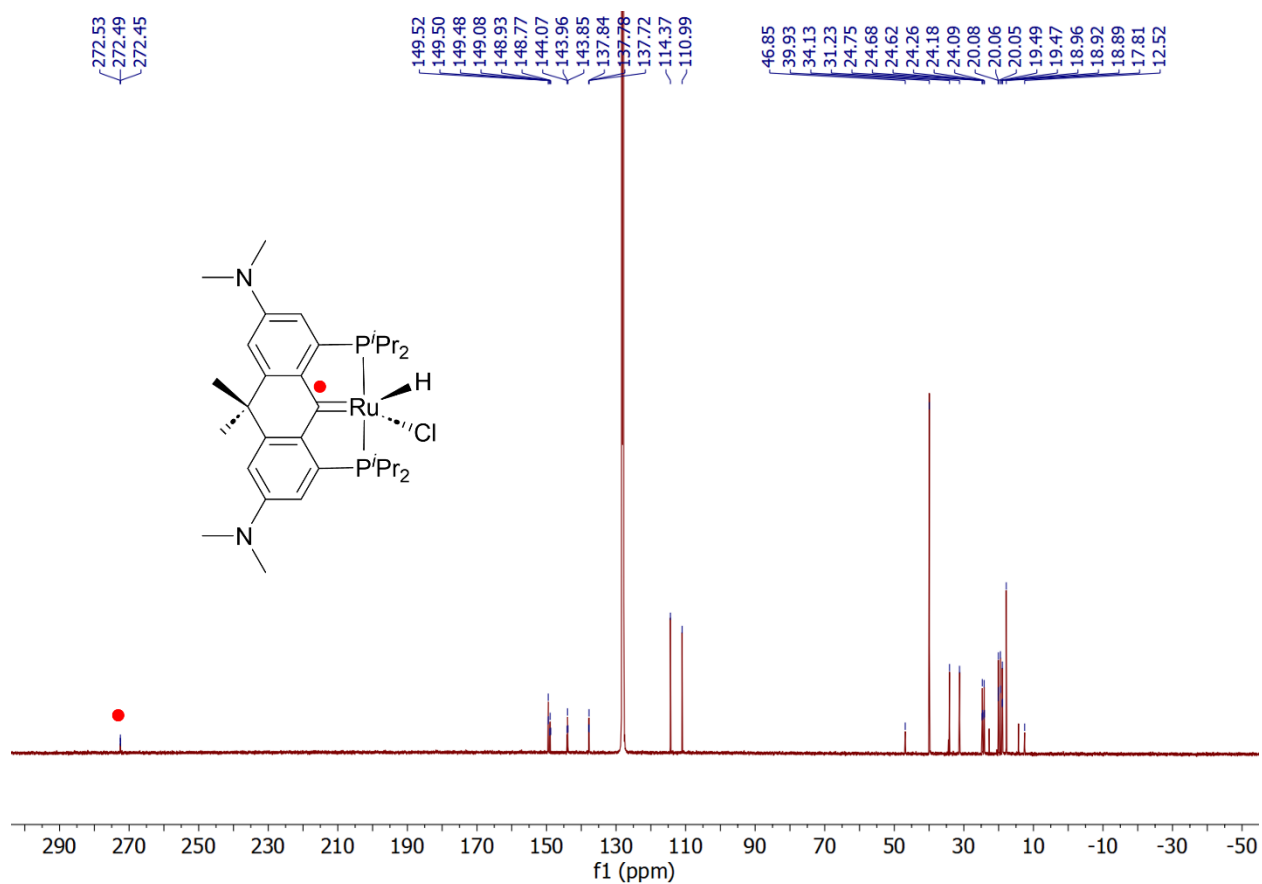


Figure S27: $^{13}C\{^1H\}$ NMR spectrum for $L_{NMe_2}Ru(H)Cl$ in C_6D_6 .

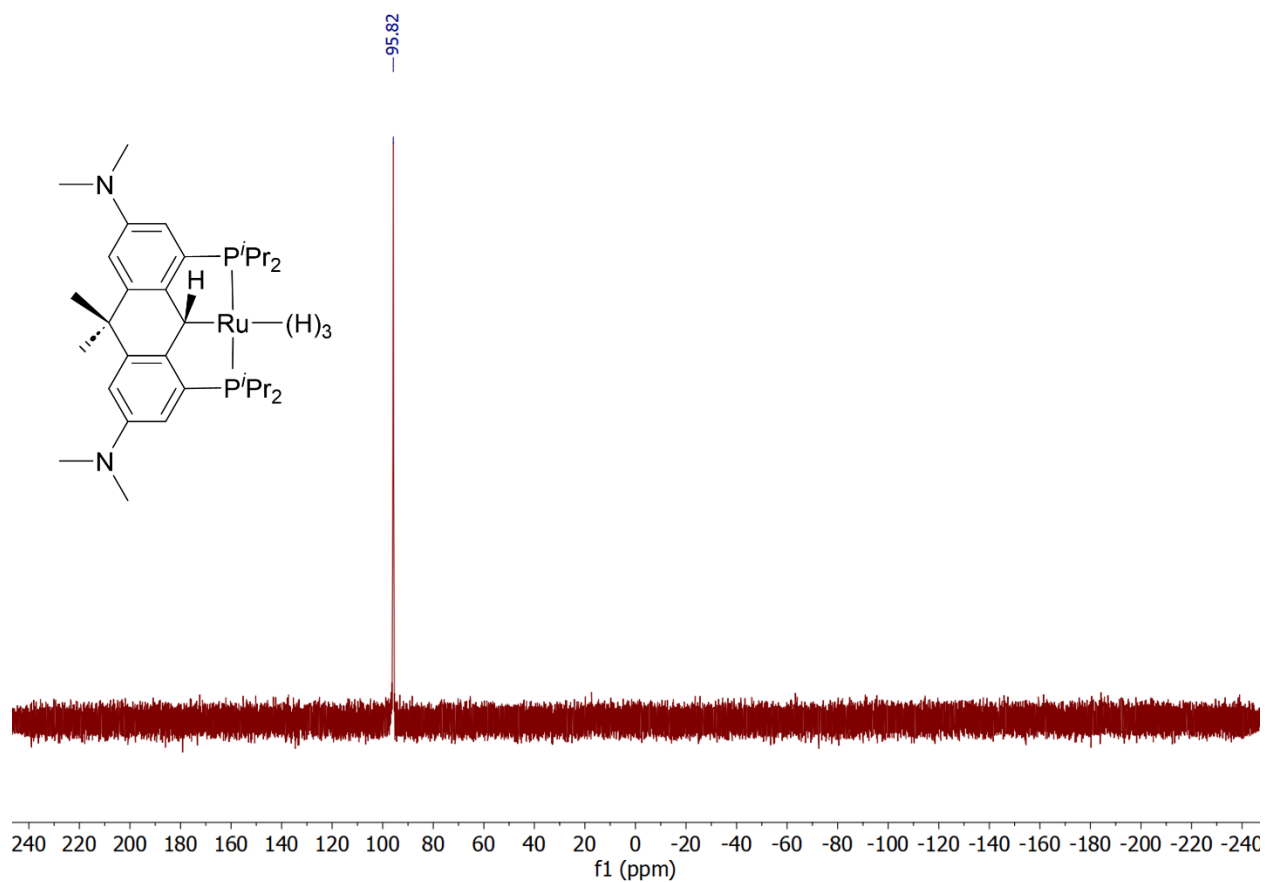


Figure S28: $^{31}\text{P}\{^1\text{H}\}$ NMR spectrum of $\text{L}_{\text{NMe}_2}\text{Ru}(\text{H})_3$ in C_6D_6 , under 1 atm of H_2 .

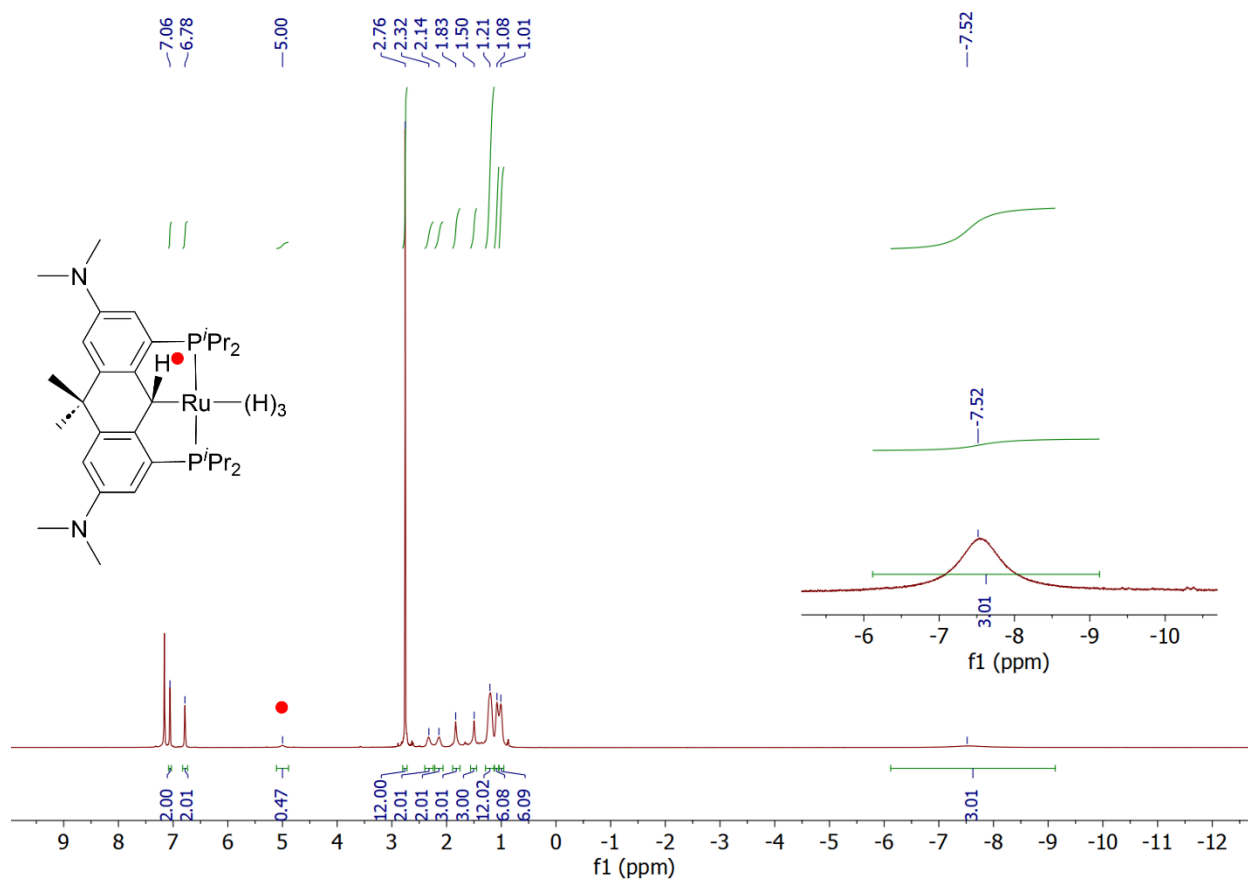


Figure S29: ^1H NMR spectrum of $\text{LNiMe}_2\text{Ru}(\text{H})_3$ in C_6D_6 , under 1 atm of H_2 .

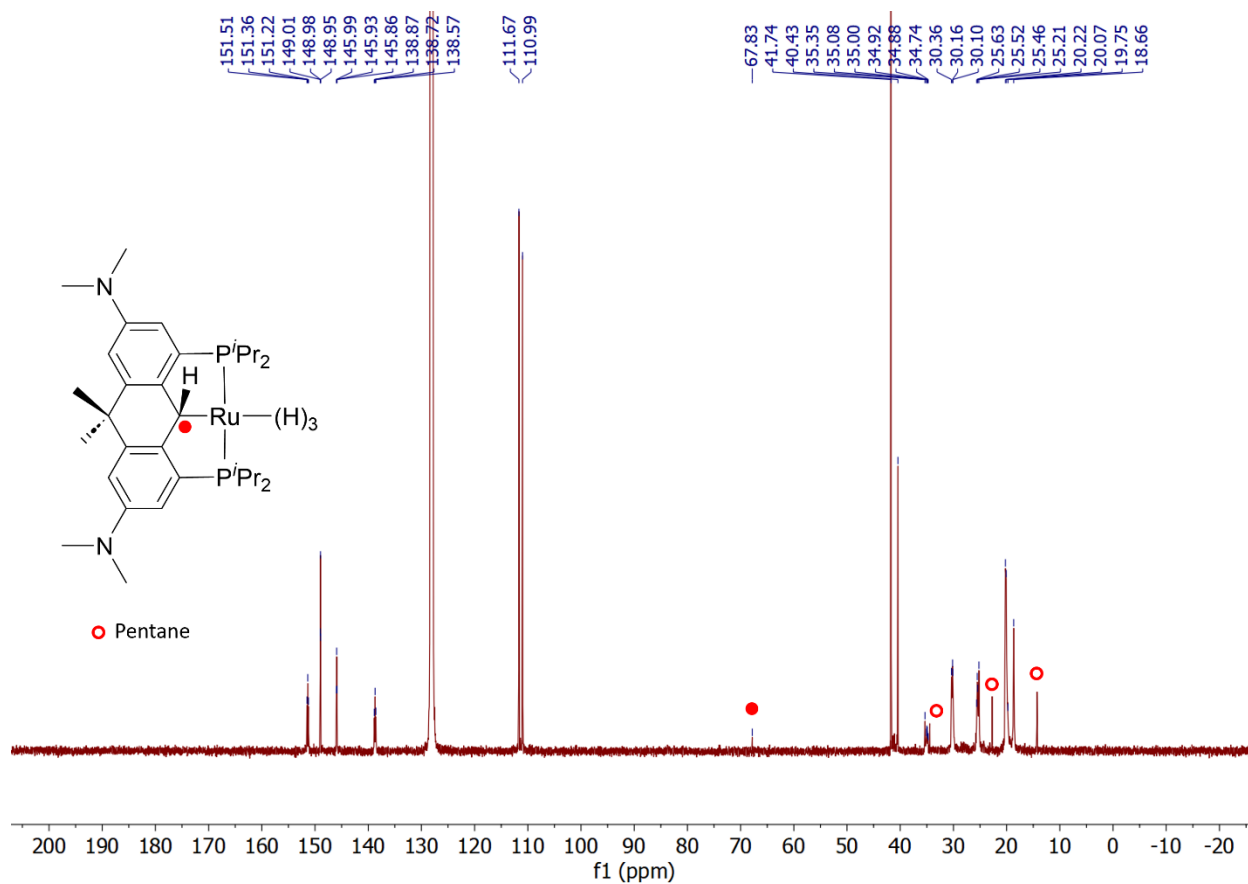


Figure S30: $^{13}C\{^1H\}$ NMR spectrum $L_{NMe_2}Ru(H)_3$ in C_6D_6 , under 1 atm of H_2

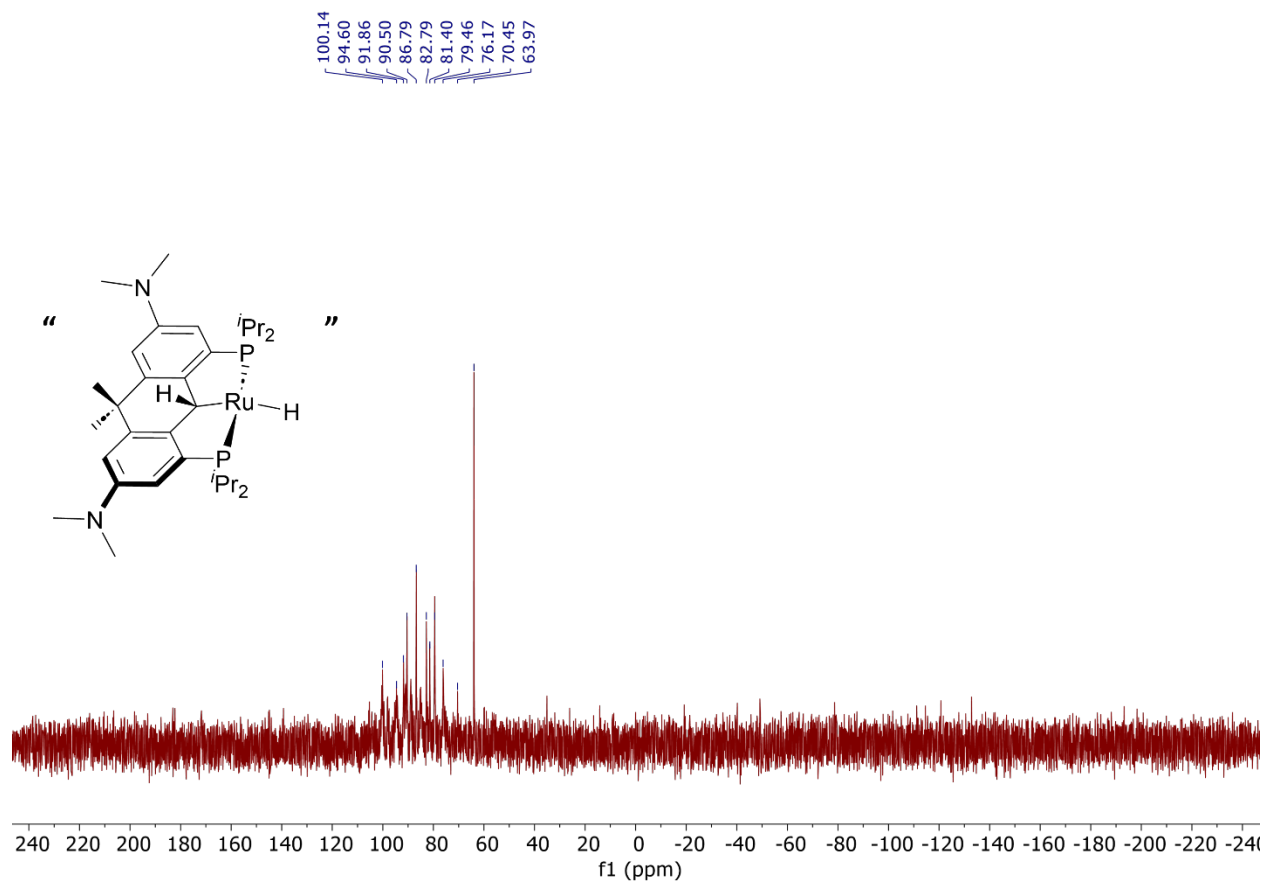


Figure S31: $^{31}P\{^1H\}$ spectrum of $L_{HNMe_2}RuH$ in C_6D_6 , under argon. Note: adding 1 atm of H_2 returns $L_{NMe_2}Ru(H)_3$ (Figure S28).

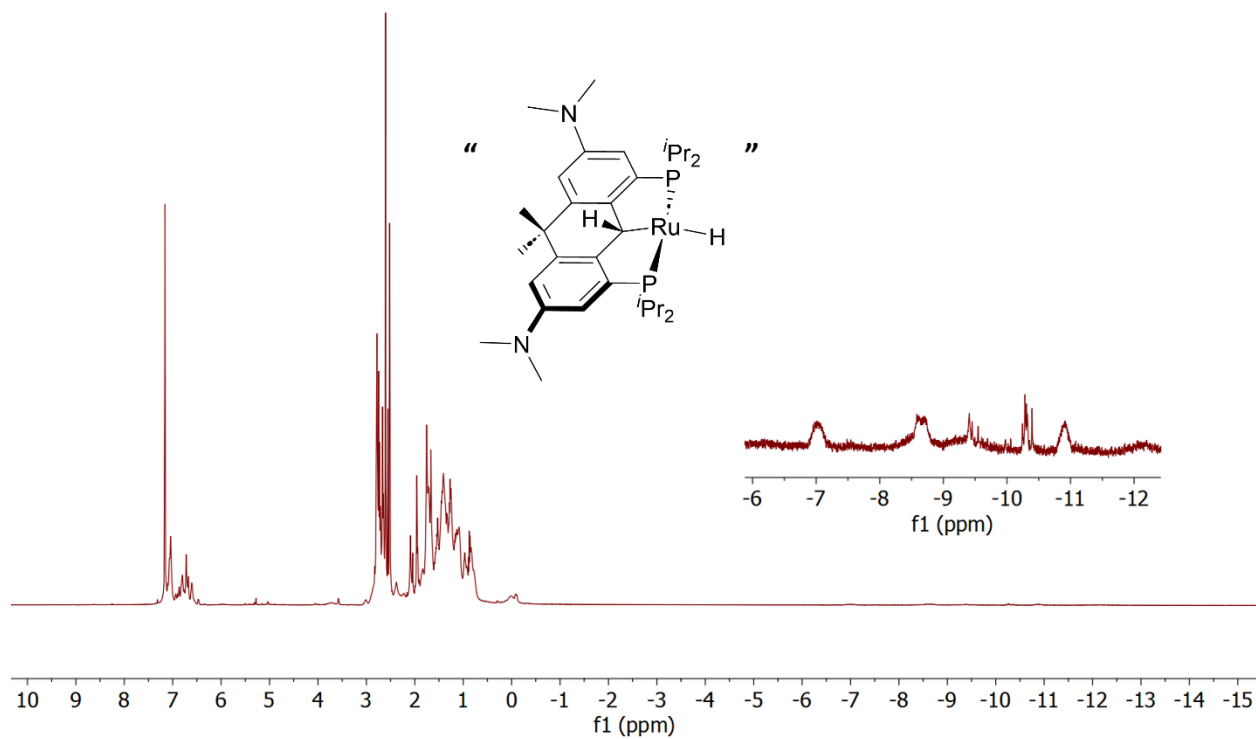


Figure S32: ^1H spectrum of $\text{L}_{\text{HNMe}_2}\text{RuH}$ in C_6D_6 , under argon. Note adding 1 atm of H_2 returns $\text{L}_{\text{NMe}_2}\text{Ru}(\text{H})_3$ (Figure S29).

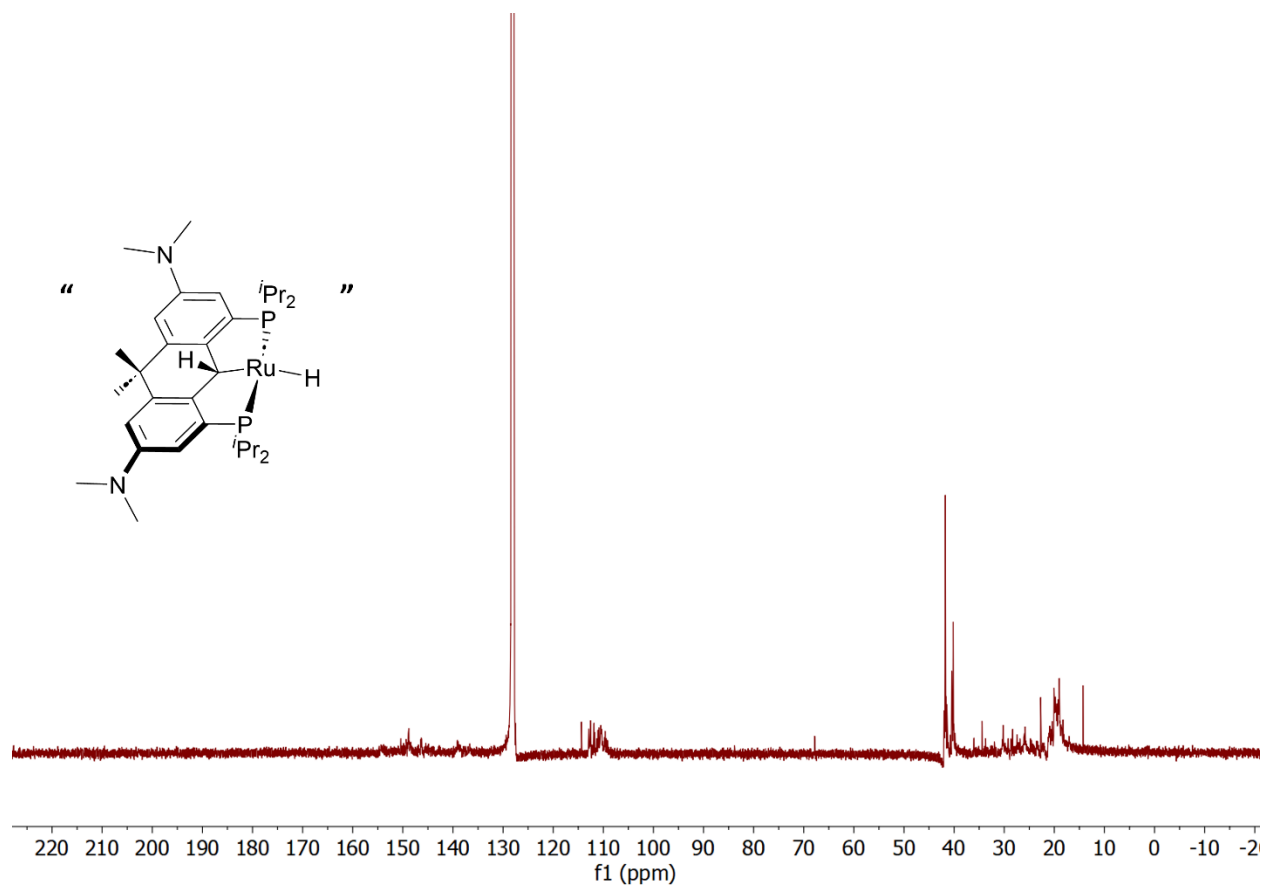


Figure S33: $^{13}\text{C}\{^1\text{H}\}$ spectrum of $\text{L}_{\text{HNMe}_2}\text{RuH}$ in C_6D_6 , under argon. Note: adding 1 atm of H_2 returns $\text{L}_{\text{NMe}_2}\text{Ru}(\text{H})_3$ (Figure S30).

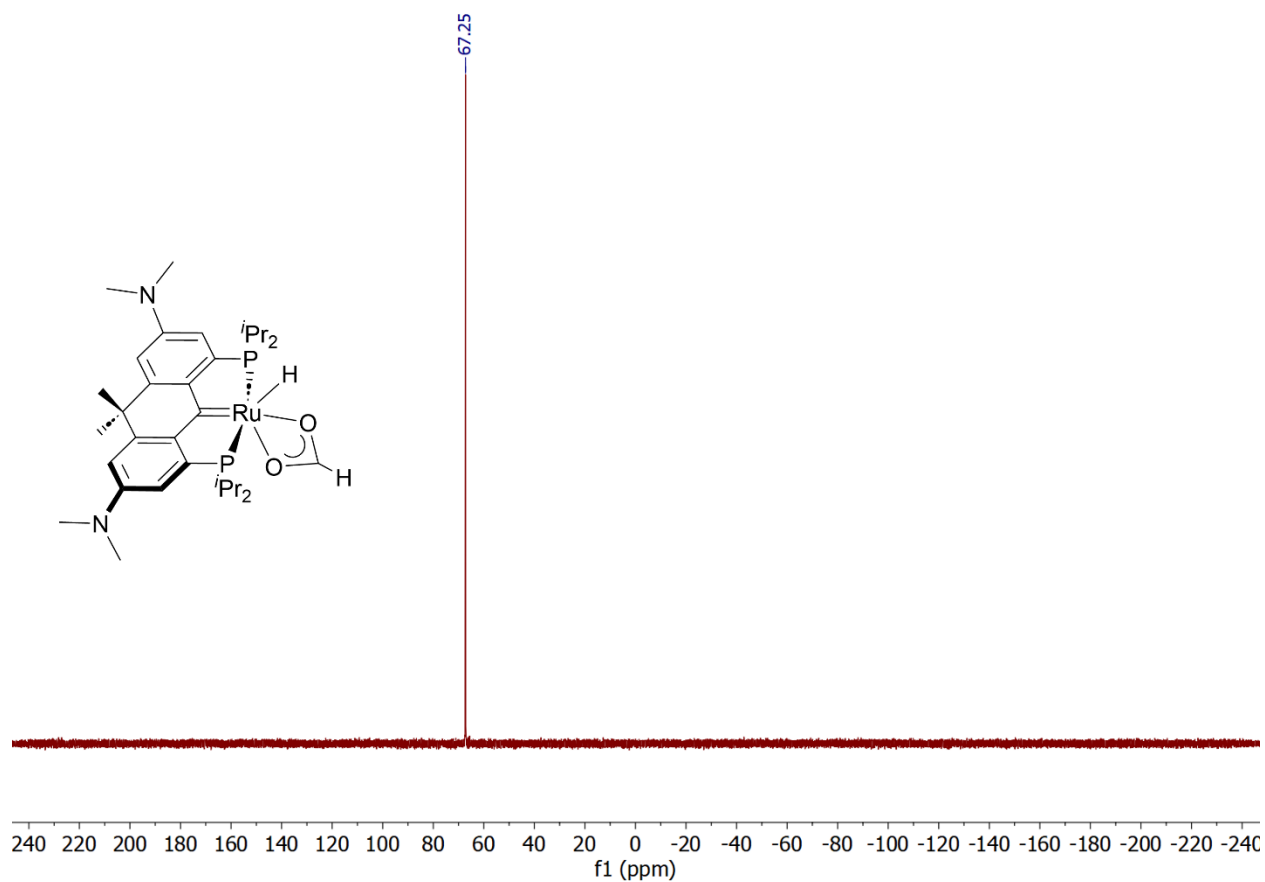


Figure S34: $^{31}\text{P}\{^1\text{H}\}$ spectrum of $\text{L}_{\text{NMe}_2}\text{Ru}(\text{H})-\kappa^2\text{-O}_2\text{CH}$ in C_6D_6 .

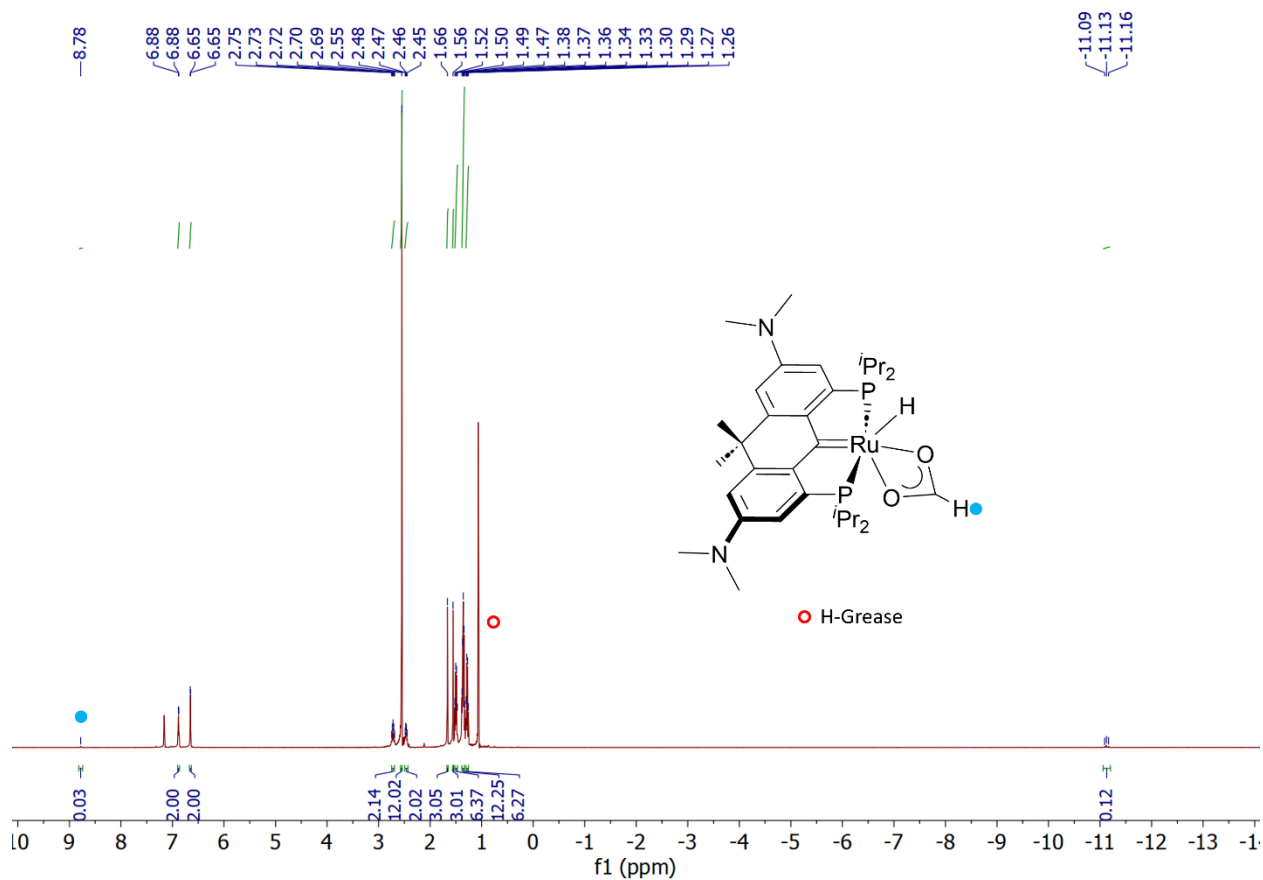


Figure S35: ^1H NMR spectrum for $\text{L}_{\text{NMe}_2}\text{Ru}(\text{H})\text{-}\kappa^2\text{-O}_2\text{CH}$ in C_6D_6 . Note proper integration of formate and hydride resonances requires prolonged d_1 times, see below.

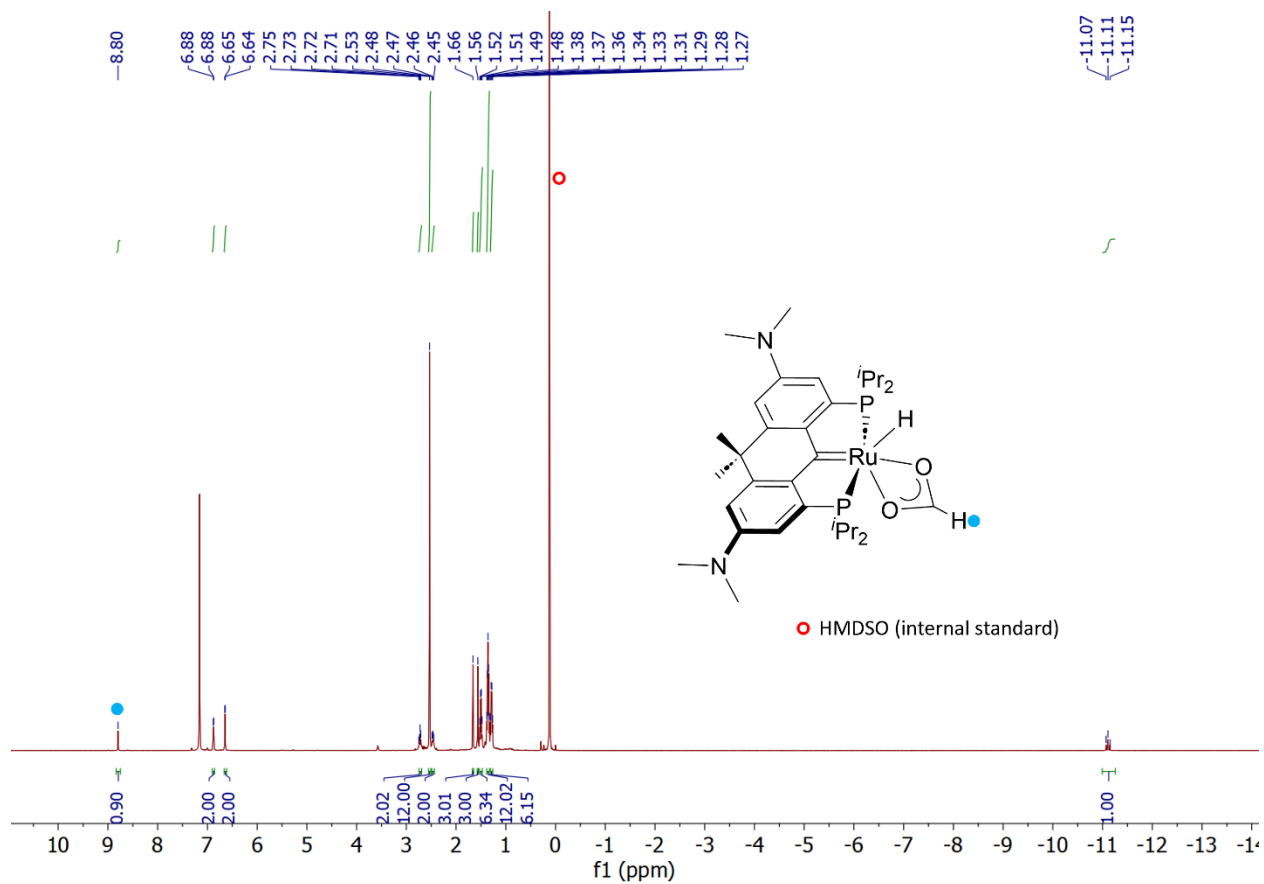


Figure S36: ^1H NMR spectrum of $\text{L}_{\text{NMe}_2}\text{Ru}(\text{H})-\kappa^2\text{-O}_2\text{CH}$ in C_6D_6 with $d1 = 30$ s and an added HMDSO standard.

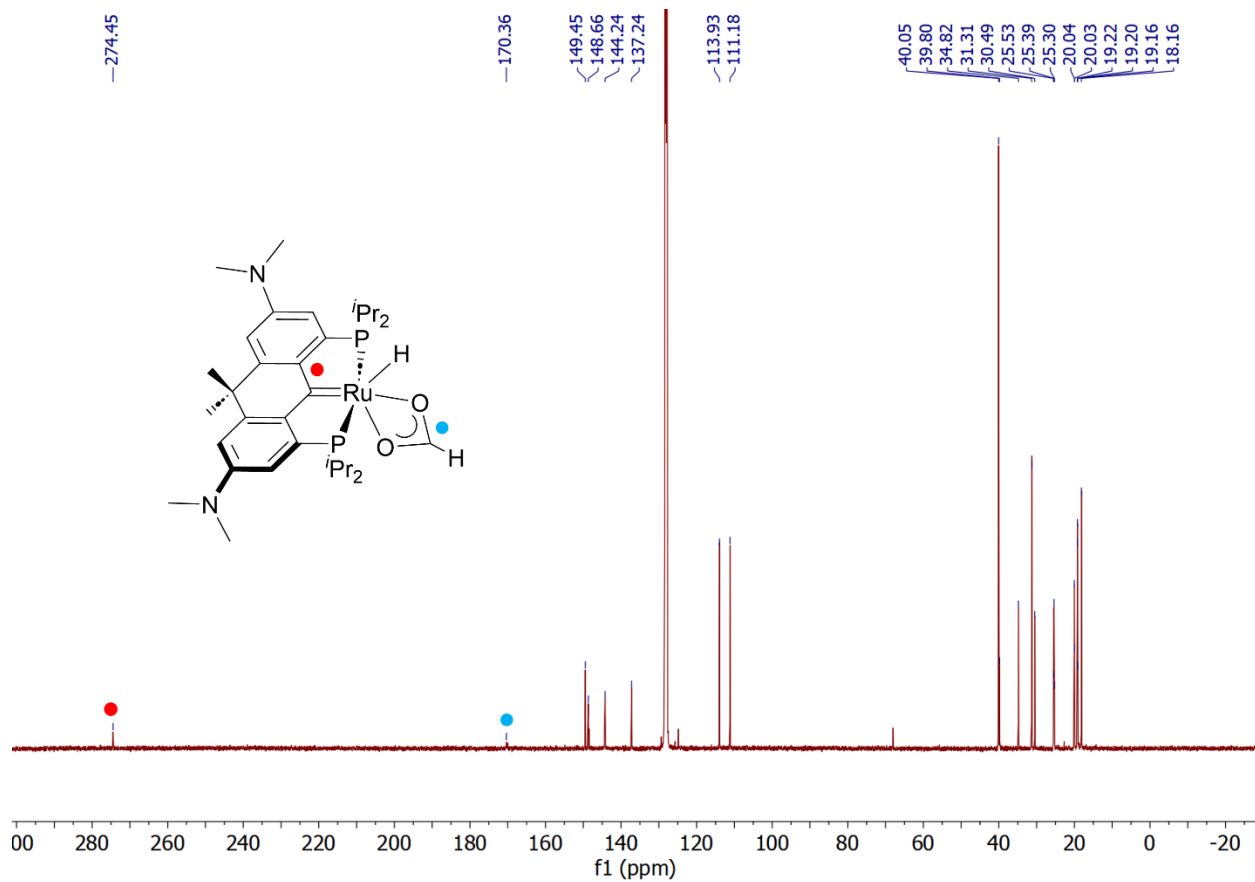


Figure S37: $^{13}C\{^1H\}$ NMR spectrum for $L_{NMe_2}Ru(H)-\kappa^2-O_2CH$ in C_6D_6 .

Variable Temperature NMR Spectra of $L_{HH}Ru(H)_3$

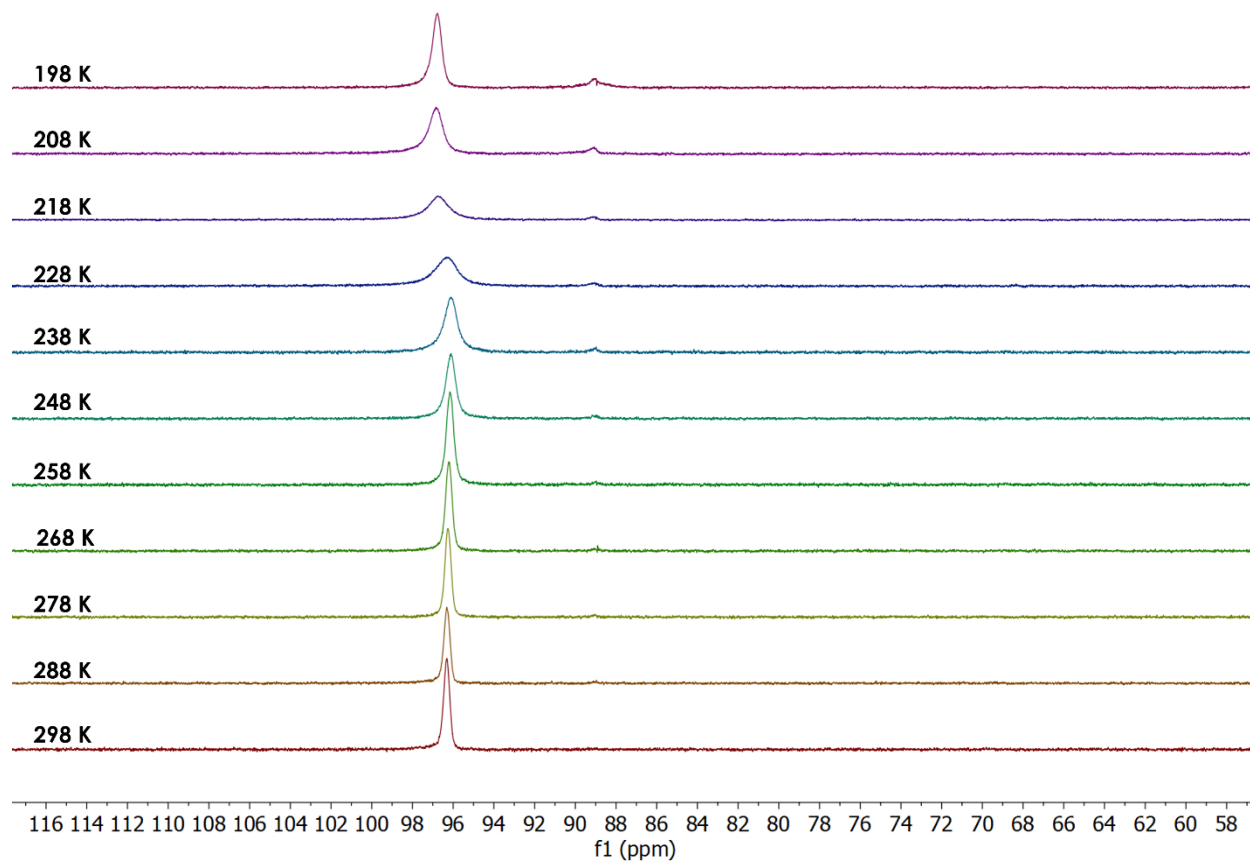


Figure S38: Variable temperature $^{31}P\{^1H\}$ spectrum for $L_{HH}Ru(H)_3$ in $toluene-d_8$, under 1 atm of H_2 .

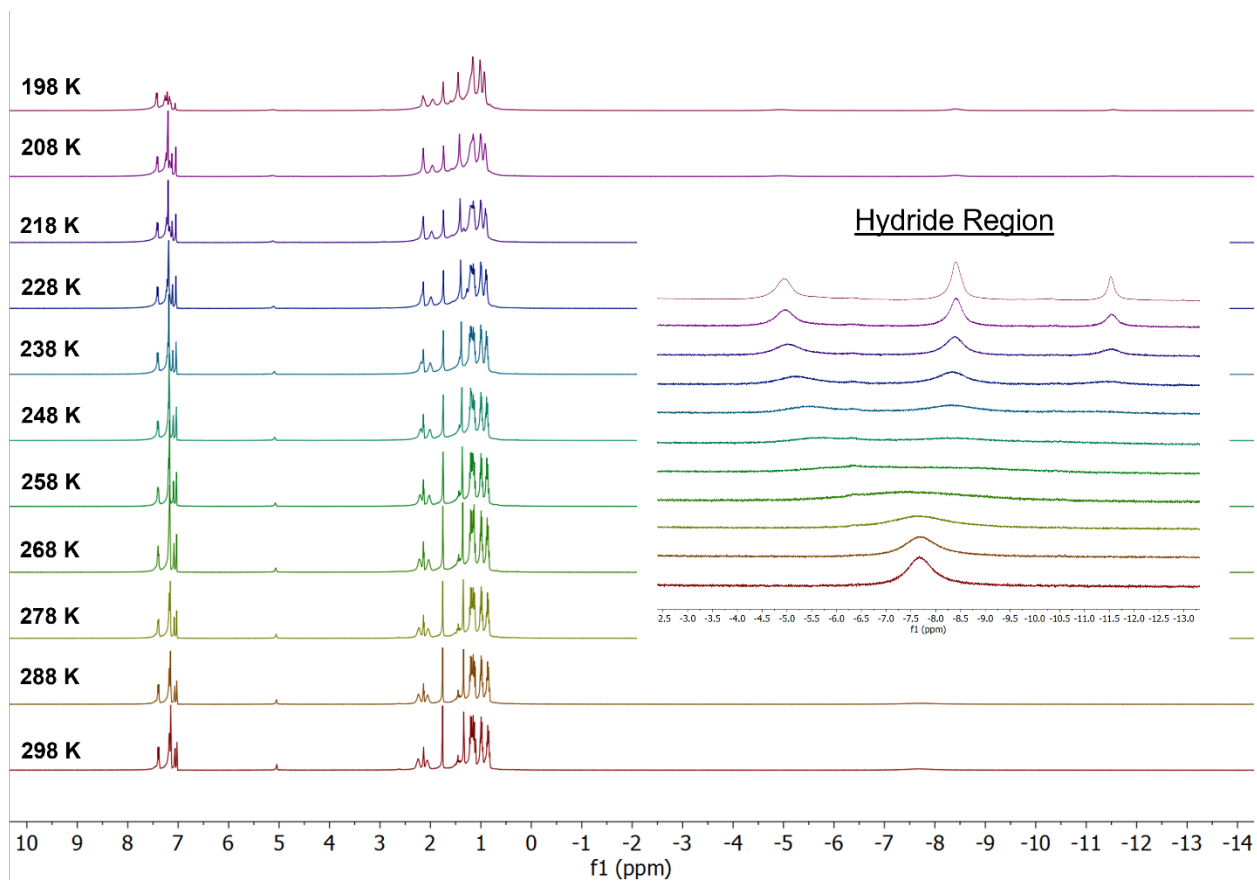


Figure S39: Variable temperature ^1H NMR Spectrum of $\text{L}_{\text{HH}}\text{Ru}(\text{H})_3$ in toluene-d_8 , under 1 atm of H_2 .

NMR Spectra of Isotopically Labeled Compounds

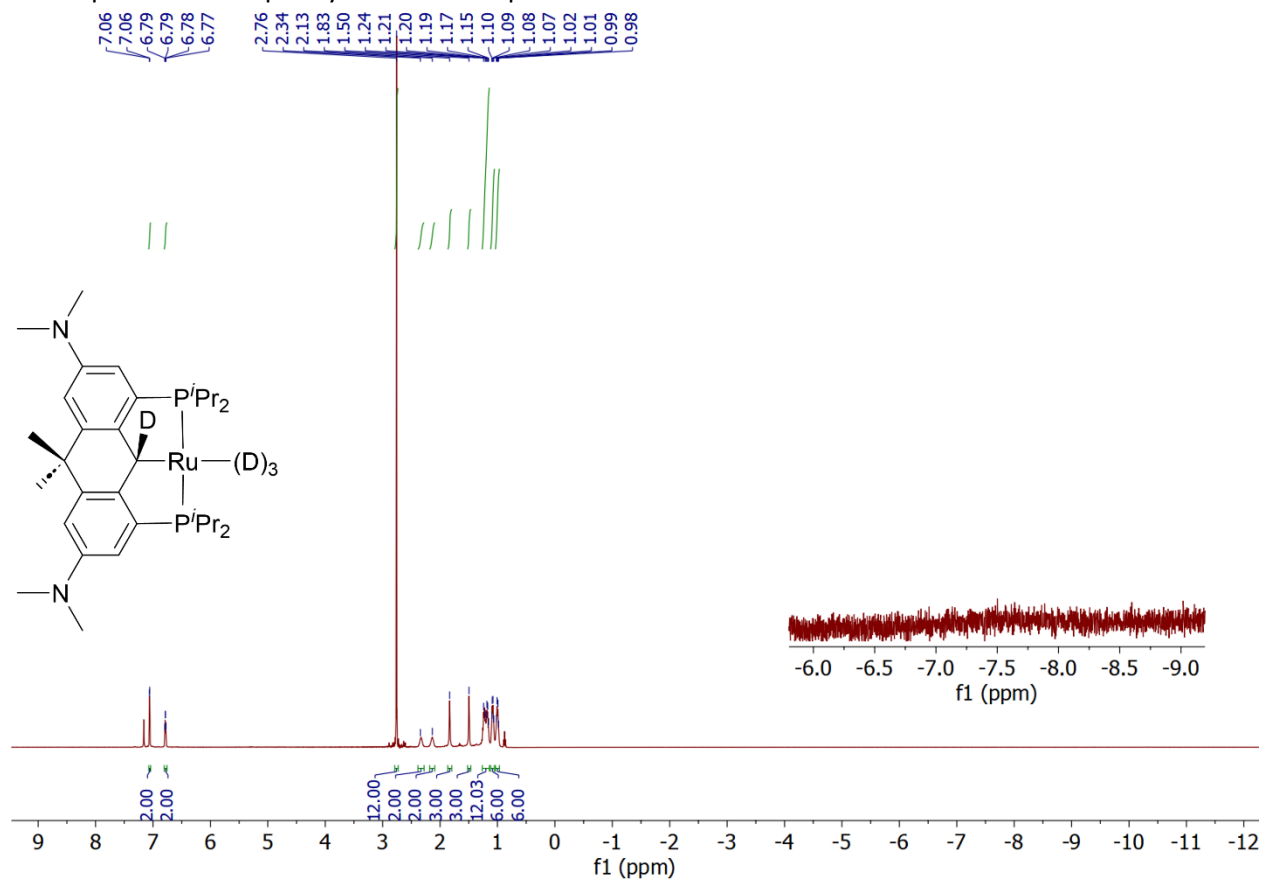


Figure S40: ^1H NMR Spectrum of $\text{L}_{\text{DNMe}_2}\text{Ru}(\text{D})_3$ in C_6D_6 , under D_2 , with an inset showing the region where the hydride resonances are observed in $\text{L}_{\text{NMe}_2}\text{Ru}(\text{H})_3$.

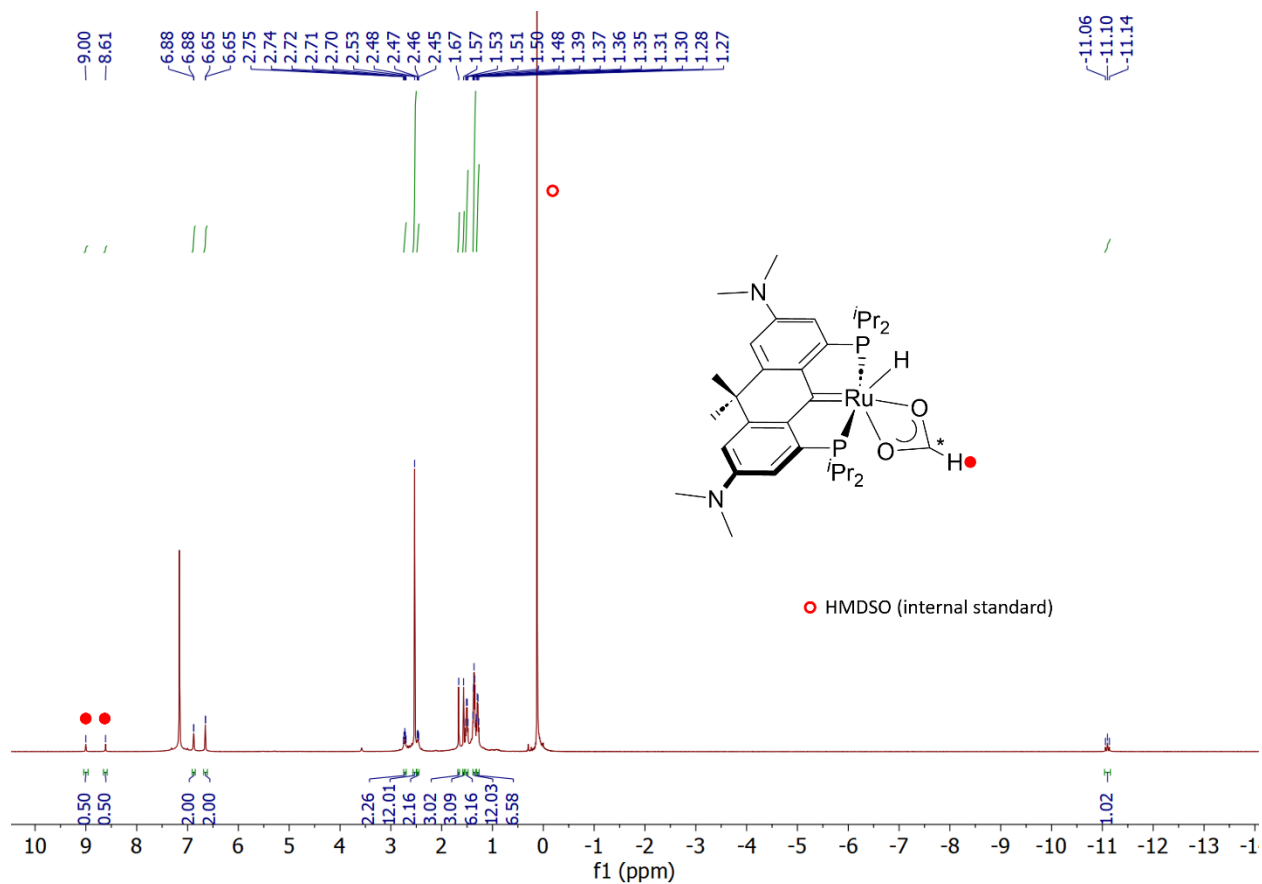


Figure S41: ^1H NMR of ^{13}C -labelled $\text{L}_{\text{NMe}_2}\text{Ru}(\text{H})\text{-}\kappa^2\text{-O}_2^{13}\text{CH}$ in C_6D_6 with $d1 = 30$ s and HMDSO standard added.

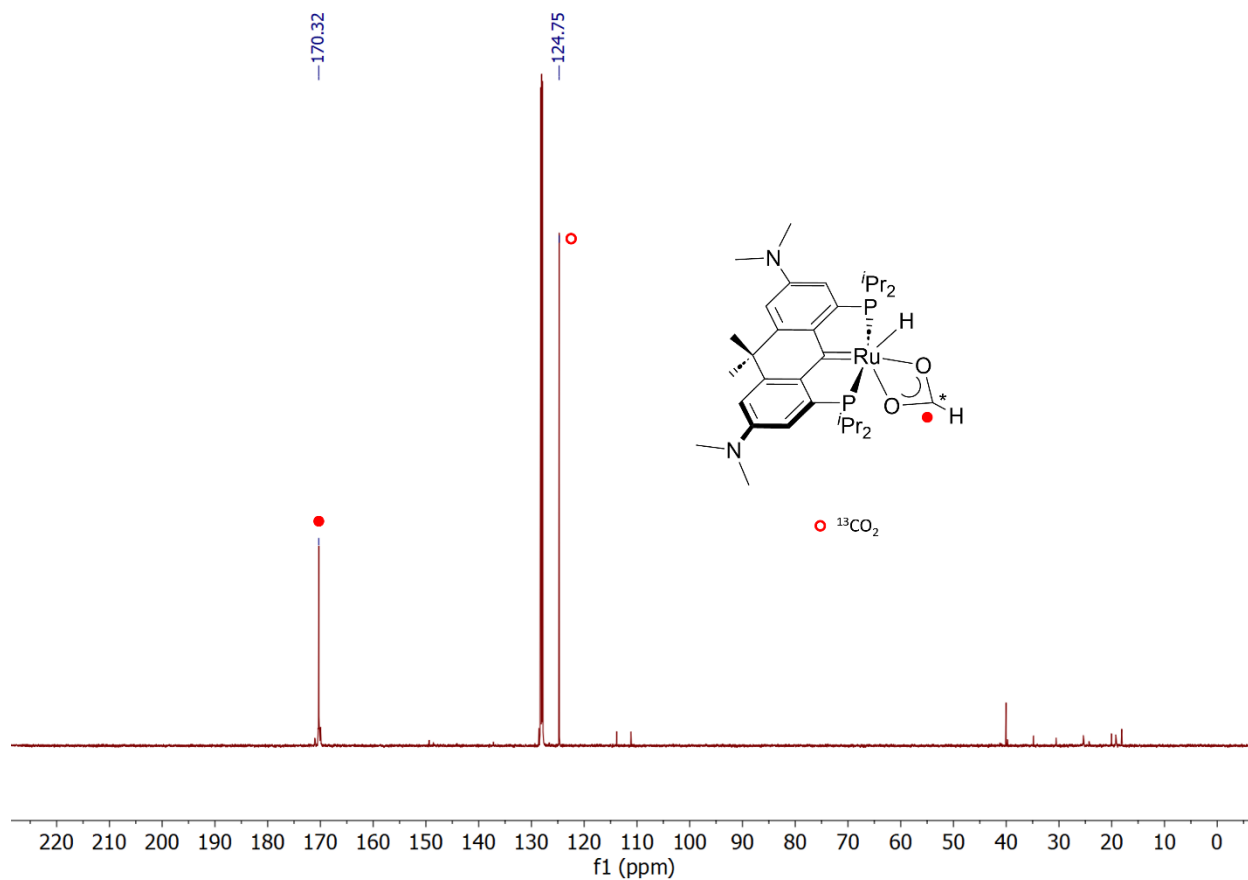


Figure S42: $^{13}C\{^1H\}$ NMR spectrum of $L_{NMe_2}Ru(H)-\kappa^2-O_2^{13}CH$ in C_6D_6 . Note: sample was prepared under an atmosphere of $^{13}CO_2$ which was not removed prior to analysis.

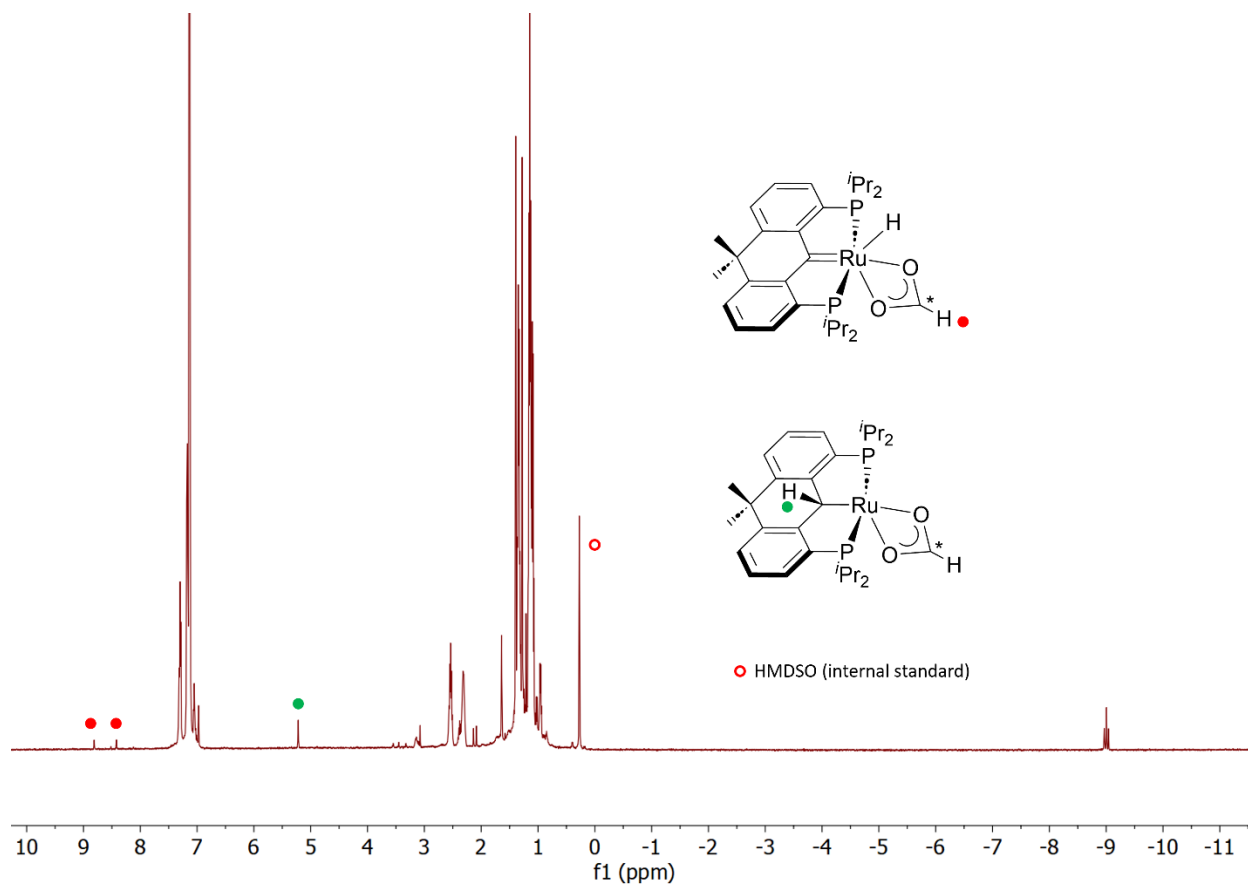


Figure S43: ^1H NMR of ^{13}C -labelled $\text{L}_\text{H}\text{Ru}(\text{H})-\kappa^2\text{-O}_2^{13}\text{CH}$ in C_6D_6 . Spectra shows both the hydride and alkyl isomer.

Determination of T_1 for $\text{L}_\text{HRu}(\text{H})_3$

T_1 values were determined using the standard inversion-recovery method on a 600 MHz spectrometer at 298 K, with the samples under an atmosphere of H_2 . Data was analysed using the TopSpin software. The values were determined to be 128 ms ($\text{R} = \text{H}$) and 61 ms ($\text{R} = \text{NMe}_2$).

Crystal Structure Determination Data

General X-ray Diffraction Collection and Refinement Information

X-ray diffraction experiments were performed by Jian-Bin Lin, Benjamin Gelfand, and Chia Yun Chang on a Bruker Smart diffractometer equipped with either Incoatec Microfocus ($\text{Cu K}\alpha$, $\lambda = 1.54178 \text{ \AA}$) or a

Siemens Fine Focus Ceramic Tube (graphite monochromated Mo K α , $\lambda = 0.71069 \text{ \AA}$) and an APEX II CCD detector. Crystals suitable for X-ray diffraction were coated in Paratone 8277 oil (Exxon) and mounted on a glass fiber before data collection. The crystals were kept at 173 K during data collection. Diffraction spots were integrated and scaled with SAINT⁸ and the space group was determined with XPREP.⁹ Using Olex¹⁰ the structure was solved with the ShelXT¹¹ structure solution program using Intrinsic Phasing and refined with the ShelXL¹² refinement package using Least Squares minimization. All non-hydrogen atoms were refined anisotropically, while hydrogen atoms (with the exception of hydrides in compounds $L_{NMe_2}Ru(H)-\kappa^2-O_2CH$, $[L_{HNMe_2}RuH]_2(\mu-N_2)$, $[L_{HH}Ru(H)(\mu-H)]_2$, and $[L_{NMe_2}RuH]_2(\mu-CO_3)$) were added in idealized positions, allowed to ride on the parent carbon atoms, and treated isotropically. The hydride Hs were unambiguously located from difference Fourier maps and isotropically refined. Generally, these H atoms were refined freely. In $[L_{HH}Ru(H)(\mu-H)]_2$, the highest residual electron density, lies along a P-Ru bond and was thus excluded from consideration as a hydrogen atom. The non-bridging hydride locations were assigned based on residual electron density in open coordination sites suggested by the geometry of the ligand. Since the electronic density is quite delocalized around the ruthenium centers, the non-bridging H and HC positions should be considered as artifacts. The bridging hydrides, HA and HB, were located by Fourier differences which were isotropically refined. In order to achieve a stable refinement and produce reasonable results, the U of the H and Ru atoms had to be restrained. Unfortunately, the highly delocalized electronic density around the ruthenium center precluded the assignment of the exact hydride location in the case of $L_HRu(H)Cl$ and $L_{NMe_2}Ru(H)Cl$. Since the hydrides were not located in the difference map, they were not included in the calculations.

Crystals for compounds $L_{NMe_2}Ru(H)-\kappa^2-O_2CH$ and $[L_{NMe_2}RuH]_2(\mu-CO_3)$ are identified to be non-merohedrally twinned. The crystal for $L_{NMe_2}Ru(H)-\kappa^2-O_2CH$ was observed to have four twin components, while the two major components accounted for roughly 90% of the crystal, according to TWINABS.¹³ The best solution came from fitting only the two major components and then using only a single component in the structural solution and refinement. Crystals of $[L_{NMe_2}RuH]_2(\mu-CO_3)$ degraded quite quickly prior to being cooled, which resulted in a diffuse reflections at low angles and minor twinning being observed. When accounting for the twin component, the TWINABS¹³ suggested that the composition was approximately 88/12. When attempting to account for the minor twin component, the residual factors and residual electron density was observed to be considerably higher than when the minor twin component was ignored and, thus, the solution and refinement were performed with just a single component.

For structures $L_{NMe_2}Ru(H)-\kappa^2-O_2CH$, $[L_{HNMe_2}RuH]_2(\mu-N_2)$, and $[L_{NMe_2}RuH]_2(\mu-CO_3)$, electron density contributions from weakly diffracting and/or diffuse solvent molecules were modelled using the SQUEEZE routine in PLATON.¹⁴

CCDC 2309264-2309271 contain supplementary crystallographic data for all structures included. These data can be obtained free of charge from The Cambridge Crystallographic Data Centre via <https://www.ccdc.cam.ac.uk/structures/>.

Additional XRD Determined Structures

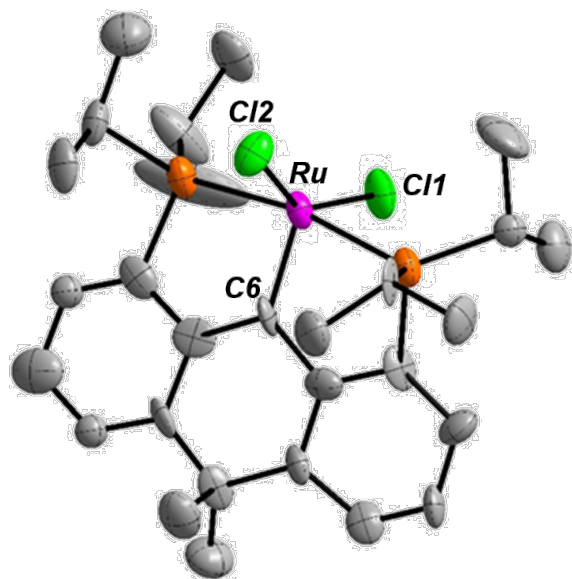


Figure S44: Structure of L_4RuCl_2 , with thermal ellipsoids drawn at 50% probability level. H atoms omitted for clarity. Selected bond lengths [Å] and bond angles [°]: Ru1-C6: 1.8749(128), Ru1-Cl1: 2.3315(54), Ru1-Cl2: 2.3400(49), Cl1-Ru1-Cl2: 146.303(174), C6-Ru1-Cl1: 98.31(5), C6-Ru1-Cl2: 115.2(5).

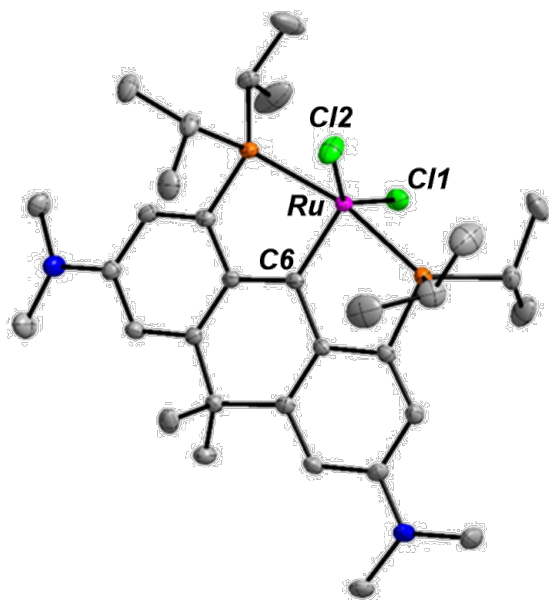


Figure S45: Structure of $L_{NMe_2}RuCl_2$, H atoms omitted for clarity. Selected bond lengths [Å] and bond angles [°]: Ru1-C6: 1.904(2), Ru1-Cl1: 2.3543(6), Ru1-Cl2: 2.3524(6); C13-Ru1-Cl1: 120.72(7), C13-Ru1-Cl2: 94.62(6).

Collection and Refinement Parameters for Included X-ray Diffraction Structures

Table S2: Relevant collection and refinement parameters for X-ray diffraction structures. Table continues in Table S3.

	L_HRu(H)Cl	L_HRuCl₂	L_{NMe₂}Ru(H)Cl	L_{NMe₂}RuCl₂
CCDC Number	2309266	2309264	2309267	2309265
Formula	C ₂₈ H ₄₀ ClP ₂ Ru	C ₂₈ H ₄₀ Cl ₂ P ₂ Ru	C ₃₂ H ₅₀ ClN ₂ P ₂ Ru	C ₃₂ H ₅₀ Cl ₂ N ₂
Formula weight	575.06	610.51	661.23	696.65
Crystal System	Orthorhombic	Orthorhombic	Monoclinic	Monoclinic
Space group	P2 ₁ 2 ₁ 2 ₁	Pbca	P2 ₁ /n	P2 ₁ /n
a(Å)	9.0549(5)	10.750(6)	11.3244(6)	19.0383(10)
b(Å)	17.2496(9)	18.8928(12)	10.9613(5)	9.7315(5)
c(Å)	17.9774(9)	27.6382(15)	31.7604(16)	18.7775(9)
α(°)	90	90	90	90
β(°)	90	90	98.1820(10)	104.432(2)
γ(°)	90	90	90	90
Volume (Å ³)	2808.0(3)	5631.5(6)	3902.3(3)	3369.1(3)
Z	4	8	4	4
Temp (K)	173	173.0	173.0	173
λ, Å	1.54178	0.71073	0.71073	0.71073
ρ _{calc} gcm ⁻³	1.360	1.440	1.269	1.373
F(000)	1196.0	2528.0	1580.0	1456.0
μ, mm ⁻¹	6.559	0.875	0.579	0.743
2θ range (°)	7.102 to 144.77	6.204 to 52	4.028 to 56.362	6.858 to 56.528
Crystal Size (mm ³)	0.2 × 0.05 × 0.05	0.15 × 0.12 × 0.08	0.27 × 0.234 × 0.134	0.384 × 0.272 × 0.21
Collected Reflections; R _σ	26865; 0.1112	43210; 0.0532	45893; 0.0343	51846; 0.0482
Unique Reflections; R _{int}	5455; 0.1364	5527; 0.0947	9559; 0.0393	8326; 0.0606
Completeness (%)	100	99.7	99.7	99.7
Data/Restraints/Parameters	5455/0/300	5527/0/319	9559/637/517	8326/0/366
R ₁ (I > 2σ(I))	0.0715	0.0455	0.0460	0.0338
wR ₂ (all data)	0.1805	0.1136	0.1235	0.0790
GoF	1.011	1.138	1.025	1.037
Largest Diffraction Peak and Hole (e/Å ³)	1.05/-1.37	1.29/-0.73	1.17/-1.04	0.58/-0.48

Table S3: Relevant collection and refinement parameters for X-ray diffraction structures.

	L_{NMe₂Ru(H)-κ²-O₂CH}	[L_{HNMe₂RuH}]₂(μ-N₂)	[L_{HHRu(H)(μ-H)}]₂	[L_{NMe₂RuH}]₂(μ-CO₃)
CCDC Number	2309270	2309269	2309268	2309271
Formula	C ₃₃ H ₅₂ N ₂ O ₂ P ₂ Ru	C ₆₄ H ₁₀₄ N ₆ P ₄ Ru ₂	C ₅₆ H ₈₆ P ₄ Ru ₂	C ₆₅ H ₁₀₂ N ₄ O ₃ P ₄ Ru ₂
Formula weight	671.77	1283.55	1085.26	1313.52
Crystal System	Monoclinic	Orthorhombic	Triclinic	Monoclinic
Space group	P2 ₁ /n	Fddd	P-1	I2/a
a(Å)	11.5021(2)	16.7299(4)	10.9417(7)	22.9521(16)
b(Å)	30.8326(7)	38.8794(11)	14.5639(11)	16.3988(9)
c(Å)	33.7646(6)	49.0089(12)	17.1311(10)	25.3602(10)
α(°)	90	90	106.789(4)	90
β(°)	93.460(1)	90	90.328(4)	107.262(2)
γ(°)	90	90	91.710(5)	90
Volume (Å ³)	11952.44(40)	31877.8(14)	2612.1(3)	9115.3(9)
Z	12	16	2	4
Temp (K)	173.0	173.0	173.0	173.0
λ, Å	1.54178	1.54178	1.54178	1.54178
ρ _{calc} g/cm ³	1.120	1.070	1.380	0.957
F(000)	4248.0	10848.0	1140.0	2768.0
μ, mm ⁻¹	4.138	4.085	6.096	3.600
2θ range (°)	3.884 to 130.166	6.028 to 133.194	5.388 to 133.524	6.51 to 134.092
Crystal Size (mm ³)	0.194 × 0.181 × 0.131	0.159 × 0.128 × 0.105	0.092 × 0.066 × 0.048	0.337 × 0.224 × 0.167
Collected Reflections; R _σ	20046;0.0973	33185; 0.0370	31954;0.1401	31623; 0.0346
Unique Reflections; R _{int}	20046;0.0909	7033; 0.0472	8889;0.1366	8059; 0.0391
Completeness (%)	98.2	99.7	96.0	99
Data/Restraints/Parameters	20046/442/1244	7033/864/480	8889/38/595	8059/164/417
R ₁ (I > 2σ(I))	0.0988	0.0835	0.0824	0.0767
wR ₂ (all data)	0.2476	0.2067	0.2073	0.2204
GoF	1.032	1.155	0.987	1.067
Largest Diffraction Peak and Hole (e/Å ³)	1.41/-1.39	0.90/-0.91	1.81/-1.12	1.70/-0.36

References

- 1 R. Tanaka, M. Yamashita and K. Nozaki, *J. Am. Chem. Soc.*, 2009, **131**, 14168–14169.
- 2 G. A. Filonenko, R. van Putten, E. N. Schulpen, E. J. M. Hensen and E. A. Pidko, *ChemCatChem*, 2014, **6**, 1526–1530.
- 3 C. A. Huff and M. S. Sanford, *ACS Catal.*, 2013, **3**, 2412–2416.
- 4 P. G. Jessop, T. Ikariya and R. Noyori, *Nature*, 1994, **368**, 231–233.
- 5 D. P. Estes, M. Leutzsch, L. Schubert, A. Bordet and W. Leitner, *ACS Catal.*, 2020, 2990–2998.
- 6 E. A. LaPierre, W. E. Piers and C. Gendy, *Organometallics*, 2018, **37**, 3394–3398.
- 7 J. D. Smith, E. Chih, W. E. Piers and D. M. Spasyuk, *Polyhedron*, 2018, **155**, 281–290.
- 8 Bruker-AXS, SAINT. SAINT, Madison, Wisconsin, USA 2017.
- 9 Bruker-AXS, XPREP. XPREP, Madison, Wisconsin, USA 2017.
- 10 O. V Dolomanov, L. J. Bourhis, R. J. Gildea, J. A. K. Howard and H. Puschmann, *J. Appl. Crystallogr.*, 2009, **42**, 339–341.
- 11 G. M. Sheldrick, *Acta Crystallogr. Sect. A*, 2015, **71**, 3–8.
- 12 G. M. Sheldrick, *Acta Crystallogr. Sect. C*, 2015, **71**, 3–8.
- 13 Bruker-AXS. TWINABS; Madison, Wisconsin, USA, 2018.
- 14 Spek, A.L. (2015). *Acta Cryst. C71*, 9-18.